SHEAR BEHAVIOR OF FRC BEAMS WITHOUT WEB REINFORCEMENT USING STEEL FIBRES WITH DIFFERENT ASPECT RATIOS

by

Murat Şen

B.S. in Civil Engineering, Pamukkale University, 2005

Submitted to the Institute for Graduate Studies in

Science and Engineering in partial fulfillment of

the requirements for the degree of

Master of Science

Graduate Program in Civil Engineering

Boğaziçi University

2009

SHEAR BEHAVIOR OF FRC BEAMS WITHOUT WEB REINFORCEMENT USING STEEL FIBRES WITH DIFFERENT ASPECT RATIOS

APPROVED BY:

Prof. Cengiz Karakoç .....
(Thesis Supervisor)

Assoc. Prof. Orhun Köksal .....

Asst. Prof. Kutay Orakçal .....

DATE OF APPROVAL: .....

To my family

ACKNOWLEDGEMENTS

Foremost, I am deeply indebted to my supervisor Prof. Cengiz Karakoç for his help, suggestions, advice, guidance, and encouragement.

I would like to convey my appreciation to Assoc. Prof. Orhun Köksal and Asst. Prof. Kutay Orakçal (members of the thesis committee) for reviewing this thesis and offering helpful comments.

I would like to thank to Osman Kaya for his help and suggestions. I want to express special thanks to technician Hasan Şenel for his assistance during the experiments.

I am grateful to Çetin Boran from Özseç Concrete Plant for his help during production and providing ready-mixed concrete used in this research. I also want to thank to Mehmet Yerlikaya from Bekaert for providing steel fibres.

Last, but not least, I would like to dedicate this thesis to my family. My special thanks go to my parents and sister for their loving support. Finally, and most importantly, I wish to thank my brother, Mustafa Şen. He has always supported and encouraged me to do my best in my studies and all matters of life.

ABSTRACT

SHEAR BEHAVIOR OF FRC BEAMS WITHOUT WEB REINFORCEMENT USING STEEL FIBRES WITH DIFFERENT ASPECT RATIOS

An experimental study was conducted on twelve beams to examine the influence of shear span-to-depth ratio (*a/d*), fibre-volume fraction, fibre aspect ratio, and concrete compressive strength on the shear behavior of beams. Two shear span-to-depth ratios (2 and 3.75), three steel fibre-volume fractions (0, 0.5, and 0.75%), two fibre types (RC-65/35-BN and RC-80/60-BN), and two concrete compressive strengths (HSC and NSC) were used in the tests. Two equal loads were symmetrically applied to the beams (four-point shear test). The applied load and the beam deflection at mid-span were recorded continuously until failure.

The results demonstrated that the cracking stress and the ultimate shear strength increased with increasing fibre volume, decreasing shear span-to-depth ratio, and increasing concrete compressive strength. The beams with long fibres exhibited higher shear strength than the beams with short fibres. As the fibre volume increased, the failure mode changed from shear to flexure. Even with small shear span-to-depth ratios, the beams with a fibre volume of 0.75% acted like beams with web reinforcement. A fibre volume fraction of 0.75% is recommended as minimum shear reinforcement for beams. The beams having a volume fraction of 0.75% failed under flexure with high displacement values at failure.

ÖZET

FARKLI BOY/ÇAP ORANINA SAHİP ÇELİK LİFLİ GÖVDE DONATISIZ BETONARME KİRİŞLERİN KESME DAVRANIŞI

Kiriş kesme açıklığının kiriş etkili derinliğine oranı (*a/d*), çelik lif oranı, lif boy-çap oranı ve beton basınç dayanımının kirişlerin kesme davranışına etkisini incelemek amacıyla bir deneysel çalışma yapılmıştır. Testlerde iki a/d oranı (2 ve 3.75), üç çelik lif oranı (0, 0.5 ve 0.75%), iki çelik lif tipi (RC-65/35-BN ve RC-80/60-BN) ve iki beton basınç dayanım seviyesi (YDB ve NDB) kullanılmıştır. Kirişler, iki eşit yükle simetrik olarak yüklenmiştir. Uygulanan yük ve kiriş orta açıklığında meydana gelen deplasman, kiriş nihai dayanımını gösterene kadar kaydedilmiştir.

Sonuçlar, çatlama gerilmesi ve kesme dayanımının, çelik lif oranı ve beton basınç dayanımının artması ve *a/d* oranının düşmesiyle arttığını göstermiştir. Uzun çelik liflerle güçlendirilmiş kirişlerin kısa olanlarla güçlendirilenlere nazaran, daha fazla kesme dayanımı gösterdiği görülmüştür. Lif oranı arttıkça, davranış kesmeden eğilmeye doğru kaymıştır. Küçük *a/d* oranları ile bile, 0.75%'lik lif içeriğinin kiriş kesme donatısı gibi görev yaptığı gözlemlenmiştir. 0.75%'lik lif içeriği kirişlerde minimum kesme donatısı olarak önerilmektedir. Bu lif oranına sahip kirişler, çok yüksek deplasman değerlerinde, eğilme kırılması ile kırılmışlardır.

TABLE OF CONTENTS

ACKNOWLEDGEMENTS iv
ABSTRACT v
ÖZET vi
LIST OF FIGURES ix
LIST OF TABLES xiv
LIST OF SYMBOLS / ABBREVIATIONS xv
1. INTRODUCTION 1
1.1. General 1
1.2. Shear Behavior and Strength of Beams without Web Reinforcement 2
1.3. The Mechanism of Shear Resistance in RC Beams without Web Reinforcement 6
1.4. Shear Design Issues of High Strength Concrete 10
1.5. Fibre-Reinforced Concrete 12
1.5.1. General 12
1.5.2. Fibre Technology 14
1.5.3. Fibre Geometries 14
1.5.4. Fibre Materials and Physical Properties 16
1.5.5. Orientation and Distribution of Fibres 16
1.5.6. Mechanics of Crack Formation and Propagation 16
1.5.7. Shear Properties 17
1.5.8. Flexural and Axial Forces 17
1.6. Objective 18
2. LITERATURE REVIEW 19
2.1. Historical Background 19
2.2. Previous Experimental and Numerical Research on Shear Strength of Beams ... 23
3. EXPERIMENTAL PROGRAM 29
3.1. General 29
3.2. Selection of Specimens 29
3.3. Material Properties 31
3.3.1. Concrete Mixture Designs 31

3.3.2. Reinforcing Steel 34
3.3.3. Steel Fibres 34
3.4. Test Set-up and Instrumentation 35
4. TEST RESULTS 38
4.1. General 38
4.2. Observations on the Specimens 38
4.2.1. Specimen BEAM-01 38
4.2.2. Specimen BEAM-02 41
4.2.3. Specimen BEAM-03 43
4.2.4. Specimen BEAM-04 45
4.2.5. Specimen BEAM-05 47
4.2.6. Specimen BEAM-06 49
4.2.7. Specimen BEAM-07 51
4.2.8. Specimen BEAM-08 53
4.2.9. Specimen BEAM-09 55
4.2.10. Specimen BEAM-10 58
4.2.11. Specimen BEAM-11 60
4.2.12. Specimen BEAM-12 62
4.3. Summary of Test Results 64
4.4. Discussion of Test Results 65
4.4.1. Influence of Shear Span-to-Depth Ratio on Shear Resistance 65
4.4.2. Effect of Concrete Strength 69
4.4.3. Influence of Fibre Type and Volume Fraction 69
4.5. Comparison of Test Results and Previous Studies 73
5. CONCLUSIONS 75
REFERENCES 77

LIST OF FIGURES

Figure 1.1. Shear force and bending moment in a simple beam 2

Figure 1.2. Pure shear and principal tensile stress 3

Figure 1.3. Directions of potential cracks in a simple beam 3

Figure 1.4. Diagonal tension failure ($3.0 < a/d < 7.0$) 4

Figure 1.5. Shear compression failure ($1.5 < a/d < 3.0$) 5

Figure 1.6. Failure mode for $a/d < 1$ 5

Figure 1.7. Variation in shear capacity with *a/d* for rectangular beams 6

Figure 1.8. Types of inclined cracks (Wang and Salmon 1979) 7

Figure 1.9. Mechanism of shear resistance (Sun and Kuchma 2007) 8

Figure 1.10. Dowel action 9

Figure 1.11. Aggregate interlock effect 10

Figure 1.12. Effect of fibres on the structural behavior (Löfgren 2005) 13

Figure 1.13. Examples of commercially available fibres (Löfgren 2005) 14

Figure 1.14. Examples of cross-sectional geometries of fibres (Löfgren 2005) 15

Figure 1.15. Examples of some typical fibre geometries (Löfgren 2005) 15

Figure 1.16. Schematic representation of different fibre composites (Löfgren 2005) . 16

Figure 1.17. Stress and deformation (a) for concrete with fibres (b) for reinforced concrete 18

Figure 2.1. Parallel chord truss model (Sun and Kuchma) 19

Figure 3.1. Production of Beams 33

Figure 3.2. Compression Testing Machine 33

Figure 3.3. Cylinder Samples 34

Figure 3.4. Test set-up 36

Figure 3.5. Test set-up in the Laboratory 36

Figure 3.6. Test set-up and instrumentation 37

Figure 4.1. Crack propagation and damaged shape of the specimen BEAM-01 39

Figure 4.2. Damaged shape of the specimen BEAM-01 39

Figure 4.3. Change in load with time (BEAM-01) 40

Figure 4.4. Load-displacement relationship for BEAM-01 40

Figure 4.5. Crack propagation and damaged shape of the specimen BEAM-02 41

Figure 4.6. Damaged shape of the specimen BEAM-02 42

Figure 4.7. Change in load with time (BEAM-02) 42

Figure 4.8. Load-displacement relationship for BEAM-02 43

Figure 4.9. Crack propagation and damaged shape of the specimen BEAM-03..... 43

Figure 4.10. Damaged shape of the specimen BEAM-03 44

Figure 4.11. Change in load with time (BEAM-03) 44

Figure 4.12. Load-displacement relationship for BEAM-03 45

Figure 4.13. Crack propagation and damaged shape of the specimen BEAM-04..... 46

Figure 4.14. Damaged shape of the specimen BEAM-04 46

Figure 4.15. Change in load with time (BEAM-04) 47

Figure 4.16. Load-displacement relationship for BEAM-04 47

Figure 4.17. Crack propagation and damaged shape of the specimen BEAM-05..... 48

Figure 4.18. Damaged shape of the specimen BEAM-05 48

Figure 4.19. Change in load with time (BEAM-05) 49

Figure 4.20. Load-displacement relationship for BEAM-05 49

Figure 4.21. Crack propagation and damaged shape of the specimen BEAM-06..... 50

Figure 4.22. Change in load with time (BEAM-06) 50

Figure 4.23. Load-displacement relationship for BEAM-06 51

Figure 4.24. Crack propagation and damaged shape of the specimen BEAM-07..... 52

Figure 4.25. Damaged shape of the specimen BEAM-07 52

Figure 4.26. Change in load with time (BEAM-07) 53

Figure 4.27. Load-displacement relationship for BEAM-07 53

Figure 4.28. Crack propagation and damaged shape of the specimen BEAM-08 54

Figure 4.29. Damaged shape of the specimen BEAM-08 54

Figure 4.30. Change in load with time (BEAM-08) 55

Figure 4.31. Load-displacement relationship for BEAM-08 55

Figure 4.32. Crack propagation on the specimen BEAM-09 56

Figure 4.33. Crack propagation and damaged shape of the specimen BEAM-09 57

Figure 4.34. Damaged shape of the specimen BEAM-09 57

Figure 4.35. Change in load with time (BEAM-09) 58

Figure 4.36. Load-displacement relationship for BEAM-09 58

Figure 4.37. Crack propagation and damaged shape of the specimen BEAM-10 59

Figure 4.38. Damaged shape of the specimen BEAM-10 59

Figure 4.39. Change in load with time (BEAM-10) 60

Figure 4.40. Load-displacement relationship for BEAM-10 60

Figure 4.41. Crack propagation and damaged shape of the specimen BEAM-11 61

Figure 4.42. Damaged shape of the specimen BEAM-11 61

Figure 4.43. Change in load with time (BEAM-11) 62

Figure 4.44. Load-displacement relationship for BEAM-11 62

Figure 4.45. Crack propagation and damaged shape of the specimen BEAM-12..... 63

Figure 4.46. Damaged shape of the specimen BEAM-12 63

Figure 4.47. Change in load with time (BEAM-12) 64

Figure 4.48. Load-displacement relationship for BEAM-12 64

Figure 4.49. Load-displacement relationship for the specimens with *a/d* = 2..... 66

Figure 4.50. Load-displacement relationship for the specimens with *a/d* = 3.75..... 67

Figure 4.51. Shear span-to-depth effect on shear resistance..... 68

Figure 4.52. Shear span-to-depth effect on cracking stress 69

Figure 4.53. Influence of volume fraction on ultimate shear stress (RC-65/35-BN) ... 70

Figure 4.54. Increase in shear strength with change in volume fraction (RC-65/35-BN) 71

Figure 4.55. Influence of volume fraction on ultimate shear stress (RC-80/60-BN) ... 72

Figure 4.56. Increase in shear strength with change in volume fraction (RC-80/60-BN) 72

LIST OF TABLES

Table 3.1. Summary of experimental program 31

Table 3.2. High strength concrete mix design 32

Table 3.3. Normal strength concrete mix design 32

Table 3.4. Characteristic properties of RC-80/60-BN and RC-65/35-BN..... 35

Table 3.5. Maximum fibre dosages 35

Table 4.1. Summary of test results 65

LIST OF SYMBOLS / ABBREVIATIONS

b_w	Width of specimens
d	Effective depth of specimens
f_{ck}	Characteristic compressive strength of concrete
$f_{t(max)}$	Maximum tensile stress
V	Shear force
V_a	Aggregate interlock force
V_c	Shear resistance of concrete
V_{cr}	Cracking shear force
V_d	Dowel action
V_f	Volume fraction
V_s	Shear reinforcement resistant
V_u	Ultimate shear force at failure
ρ	Longitudinal reinforcement ratio
σ_c	Compressive stress
σ_t	Tensile stress
τ_s	Shear stress
v	Shear stress
a/d	Shear span-to-effective depth ratio
HSC	High strength concrete
NSC	Normal strength concrete

1. INTRODUCTION

1.1. General

Shear force is the rate of change in bending moment along the span. Reinforced concrete structural members have to resist shearing forces. These forces may act alone or in combination with flexure and axial load. An exact analysis of shear strength is quite complex. The main obstacle to the shear problem is the large number of parameters involved, some of which may not be known. The wide study of the behavior of reinforced concrete members has been conducted to understand the various modes of failure that could occur due to possible combination of shear and bending moment acting at a given section. These studies have clarified the shear failure mechanism to the extent that acceptable conclusions are now assembled in the design codes.

The failure of the beams dominated by shear is induced by cracks outside the central section of the beam. Although the bending moment is the maximum in the central section, the cause of failure is the shear force in the end region of the beam where the cracks appeared causing failure. It is to be noted that in the central section, there is pure bending (no shear force). It is felt that the shear force, or the shear stress, must be responsible for such a failure.

The usual arrangement for investigating shear failure is that of a beam subjected to symmetrically placed two equal concentrated loads with a distance of ‘a’ (shear span). It has the advantage of combining two different test conditions that are no shear force in between the two loads and constant shear force in the two end regions or shear spans.

The transfer of shear in reinforced concrete members occurs by a combination of the shear resistance of the uncracked concrete (V_c), aggregate interlock force (V_d), dowel action (the resistance of the longitudinal reinforcement to a transverse force, V_a), arch action and shear reinforcement resistance (V_s - not available in beams without web reinforcement). Shear transfer in reinforced concrete beams depends heavily on the tensile and compressive strength of the concrete. Therefore, it is clear that a shear failure is non-

ductile generally. When ductility is essential, the shear strength of the member must exceed the shear force corresponding to the maximum flexural strength it could possibly develop.

It is well-known that the use of steel fibres improves the ductility of concrete and fracture energy. Most of the properties of fibrous concrete can be used to enhance the behavior of concrete members reinforced with conventional bar reinforcement. This phenomenon is transferable to the shear strength of concrete. The use of steel fibres is particularly attractive if conventional stirrups can be eliminated, which reduces reinforcement congestion. Fibre-reinforced concrete extends the versatility of concrete as a construction material, offers a potential to simplify the construction process and, when combined with self-compacting concrete, signifies an important step towards industrial construction.

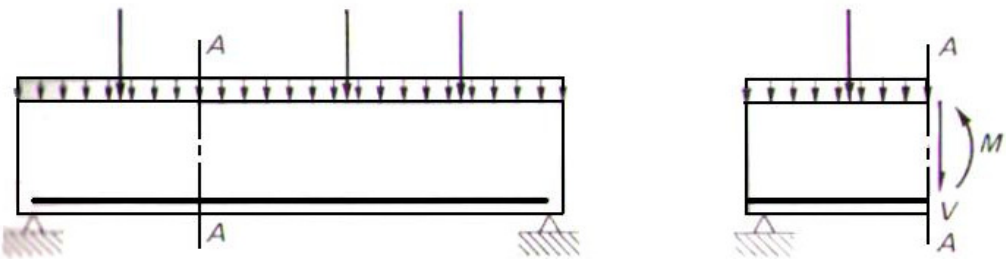

Figure 1. 1. Shear force and bending moment in a simple beam

1.2. Shear Behavior and Strength of Beams without Web Reinforcement

Considering a simple beam, the bending moment at a cross-section of the beam causes compressive stresses in the concrete above the neutral axis, and tensile stresses in the longitudinal reinforcement and in the lower part of concrete. The summation of the vertical shear stresses in the section must be equal to the shear force to satisfy vertical equilibrium. At the lower part of the beam, there is nearly a state of pure shear which gives rise to a tensile stress of equal magnitude on a 45° rotated plane. This diagonal tension is the main cause of inclined cracking. Therefore, the shear failures in beams are actually tension failures at the inclined cracks [1].

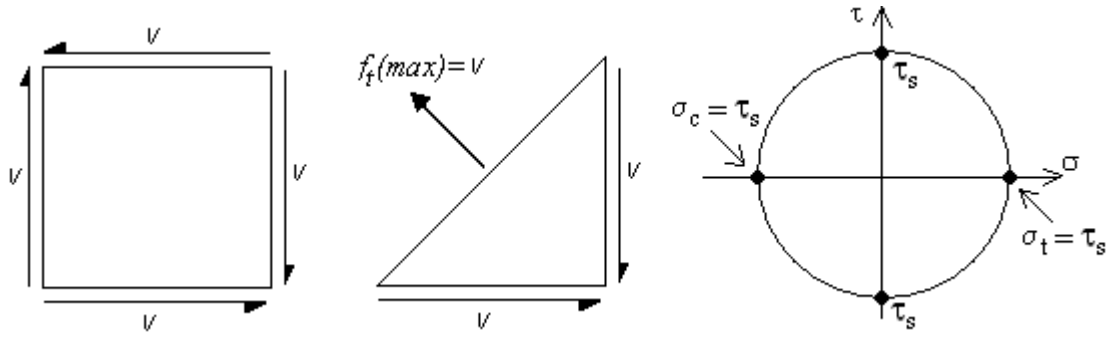

Figure 1.2. Pure shear and principal tensile stress

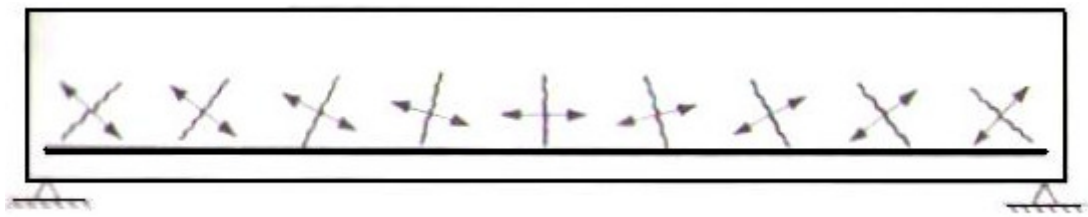

Figure 1.3. Directions of potential cracks in a simple beam

The behavior and strength of reinforced concrete beams is influenced by the dimensionless shear-span-to-depth ratio, *a/d*. When *a/d* ratio is large, i.e. greater than 7.0 or 8.0, then the behavior will be dominated by flexure. Of course this depends on the percentage of longitudinal steel but for normal percentages, a beam having an *a/d* greater than 7.0 or 8.0 will fail in flexure by yielding of the tension steel and then crushing of concrete in the compression zone. In such beams although the flexural cracks in the shear span are slightly inclined, no diagonal cracks form.

Beams with $3.0 < a/d < 7.0$ fail by the formation of a diagonal crack at loads lower than the ones corresponding to flexural capacity. Typical crack pattern for such a beam is shown in Figure 1.4. At early stages of loading flexural cracks will appear at zones of maximum moment. As the load is increased, these flexural cracks progress vertically and new cracks open in the shear span. These flexural cracks are almost vertical even in the shear span. As the load is increased, some of the flexural cracks in the shear span are inclined toward the load as they progress upward (marked as 2 and 3 in the figure). At a certain stage, one of these inclined cracks kicks back, i.e. inclined crack progresses downward to the level of tension steel (marked as 4 in the figure). The inclined crack that

extends from the level of the steel to the compression zone is called *true diagonal crack.* With the formation of this diagonal crack, redistribution takes place and the stress in longitudinal steel increases significantly. As the load is increased, the beam fails suddenly with the diagonal crack extending into the compression zone (marked as 5 and along the longitudinal steel (marked as 6). This type of failure, which is very sudden, extremely brittle and destructive is called *diagonal tension failure.*

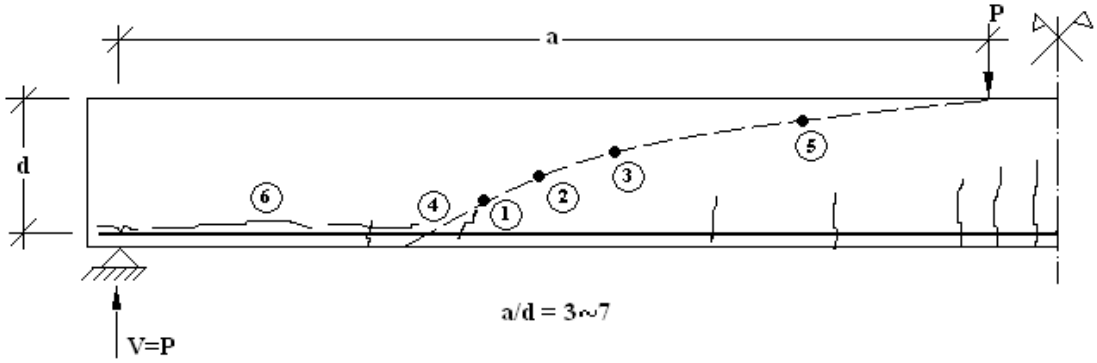

Figure 1.4. Diagonal tension failure (3.0 < *a/d* < 7.0)

If the shear span is decreased (1.5 < *a/d* < 3.0), the type of failure changes. Similar to the previous case, initial cracks are flexural cracks that are almost vertical. As the load is increased, cracks in the shear span progress upward and start to get inclined as shown in Figure 1.5. When the inclined crack reaches the level of longitudinal steel and extends toward the load (points marked as 3 and 4 in the figure), redistribution takes place. At this stage, diagonal crack is fully developed. However, different from the previous case (3.0 < *a/d* < 7.0) further increase in the load doesn't lead to failure. The beam continues to carry the increasing load with fully developed diagonal cracks. Finally, failure takes place by crushing of concrete in the compression zone (marked as 5 in the figure). This type of failure is called *shear-compression failure.* In both diagonal tension and shear-compression failures, the maximum moment reached is below the flexural capacity. In the case of larger shear span (3.0 < *a/d* < 7.0), the diagonal cracking load is the same as the failure load. However, in beams with shorter spans (1.5 < *a/d* < 3.0), failure load is greater than the diagonal cracking load. Therefore, although the failure is still brittle, it is not as sudden and brittle as the diagonal tension failure.

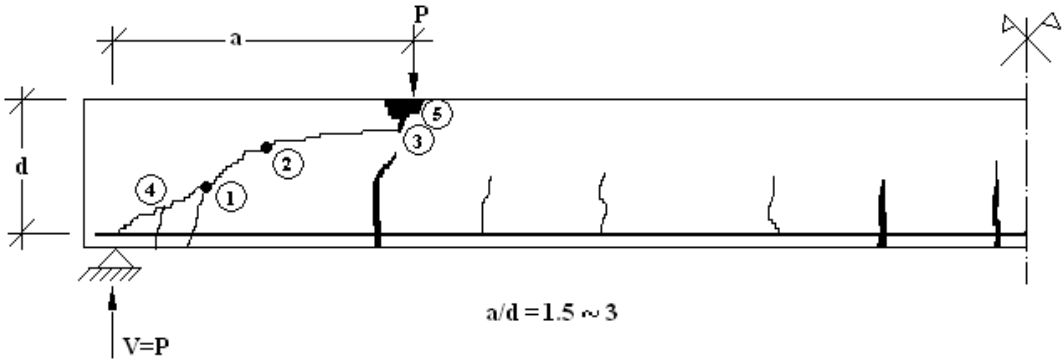

Figure 1.5. Shear compression failure (1.5 < *a/d* < 3.0)

In beams with very short shear spans, *a/d* < 1.0, failure due to principal tensile stresses is not possible. As shown in Figure 1.6, in such cases, the load is directly transferred to the support with a compression strut forming in the web. In this case, the beam reaches its flexural capacity. The final failure can take place by crushing of concrete in the compression zone, crushing of the web or by anchorage failure near the support. Members with such a short shear span behave like a *tied arch* rather than a beam. Therefore, the longitudinal steel acting as a tie rod creates severe anchorages problems in the vicinity of the reaction [3].

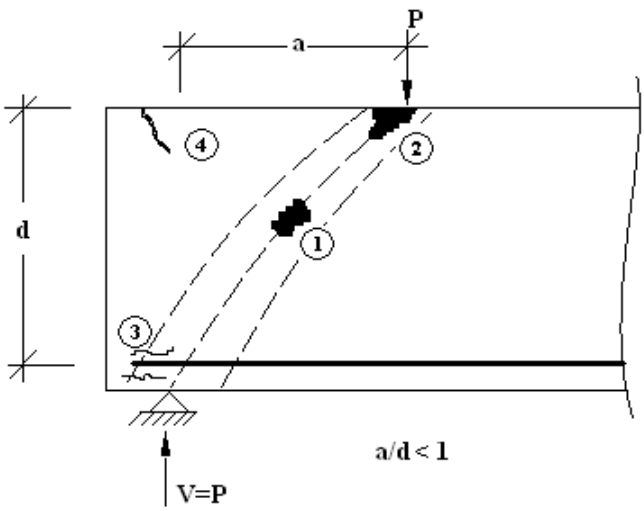

Figure 1.6. Failure mode for *a/d* < 1

When shear factors other than shear span-to-depth ratio are kept constant, the variation in shear capacity may be illustrated by Figure 1.7 using the results for rectangular

beams. From the figure, four general categories of failure mentioned above may be established.

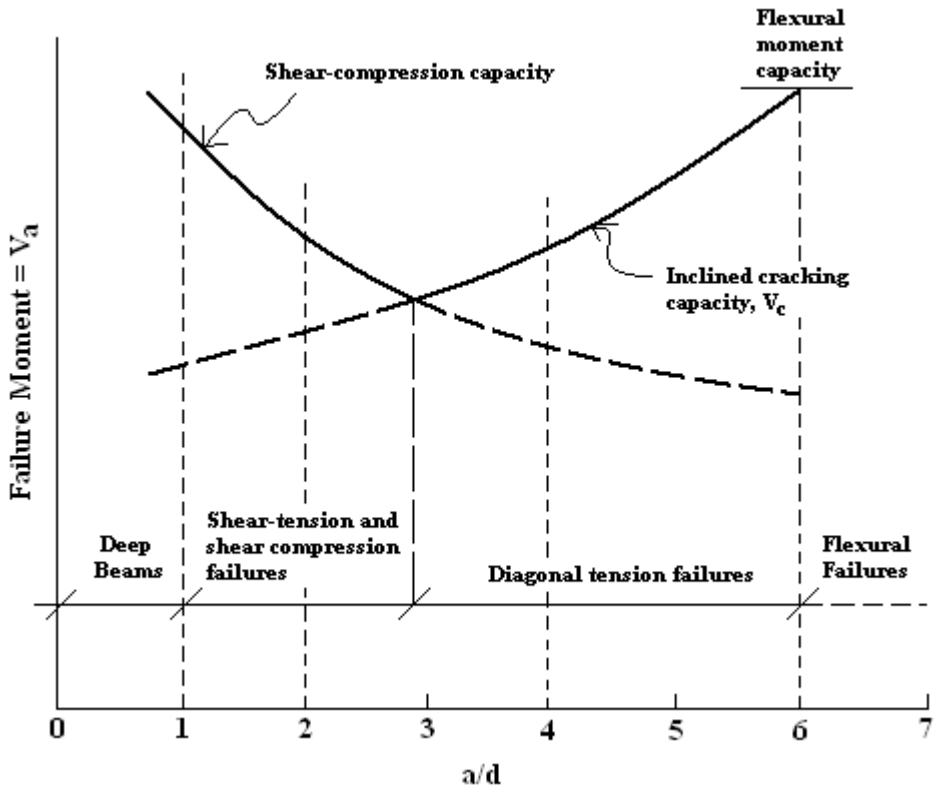

Figure 1.7. Variation in shear capacity with *a/d* for rectangular beams

1.3. The Mechanism of Shear Resistance in RC Beams without Web Reinforcement

In a reinforced concrete beam, shear and flexure create a biaxial state of stress. Cracks form when the tensile stresses are higher than the tensile strength of the concrete. In a section of high shear force, diagonal tension may be generated at 45° to the neutral axis of the member. This may result in inclined cracks. Generally, these inclined cracks are extensions of flexural cracks. Either the beam collapses immediately after the formation of diagonal cracks, or a new shear carrying mechanism develops.

In cracking in the webs of reinforced concrete beams may develop either in the absence of flexural cracks in the vicinity or as an extension of a previously developed flexural crack. An inclined crack occurring in a beam that was previously uncracked due to flexure is known a web-shear crack. Web shear cracks are relatively rare, particularly in

non-prestressed beams. These cracks occur in thin-webbed I-shaped beams having relatively large flanges, common only in prestressed concrete construction. On the other hand, an inclined crack originating at the top of and becoming an extension to a previously existing flexural crack is known as a flexure-shear crack. These cracks are the usual type found in both reinforced and prestressed concrete. In non-prestressed reinforced concrete beams, flexural cracking is expected under service load. The critical flexural crack is referred to as the "initiating crack". The flexural cracks, usually extending approximately vertically into the beam, cause no distress to the beam until a critical combination of flexural and shear stress develops near the interior extremity of one of the cracks. The inclined cracks then form. The rate of transformation of the initiating flexural crack into the flexure-shear crack depends on the rate of growth and height of flexural cracks, as well as the magnitude of shear stresses acting near the tops of flexural cracks [1].

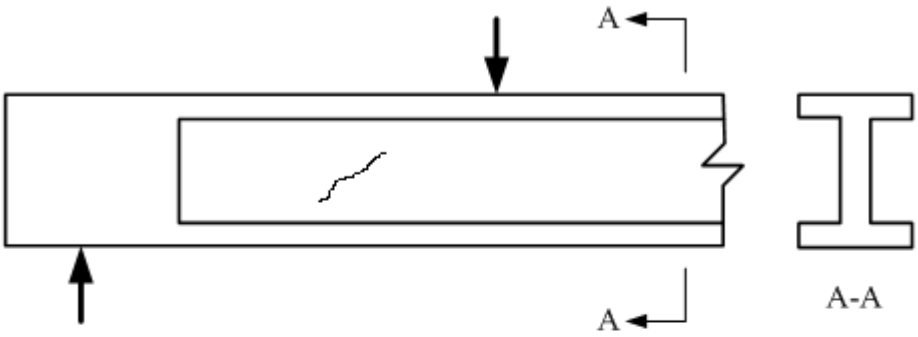

(a) Web-shear crack

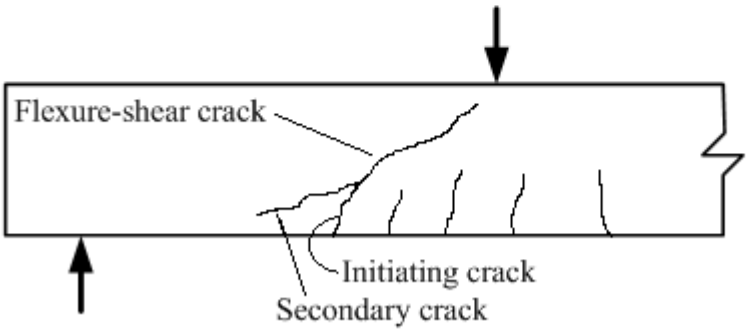

(a) Flexure-shear crack

Figure 1.8. Types of inclined cracks (Wang and Salmon 1979)

The transfer of shear in reinforced concrete members occurs by a combination of the following mechanisms, as shown in Figure 1.9.

(a) Shear resistance of uncracked concrete, V_c.
(b) Aggregate interlock (or interface shear transfer) force, V_a, tangentially along a crack, and similar to a frictional force due to irregular interlocking of the aggregates along the rough concrete surfaces on each side of the crack.
(c) Dowel action, V_d, the resistance of the longitudinal reinforcement to a transverse force.
(d) Arch action on relatively deep beams.
(e) Shear reinforcement resistance, V_s, from vertical or inclined stirrups (not available in beams without shear reinforcement) [1].

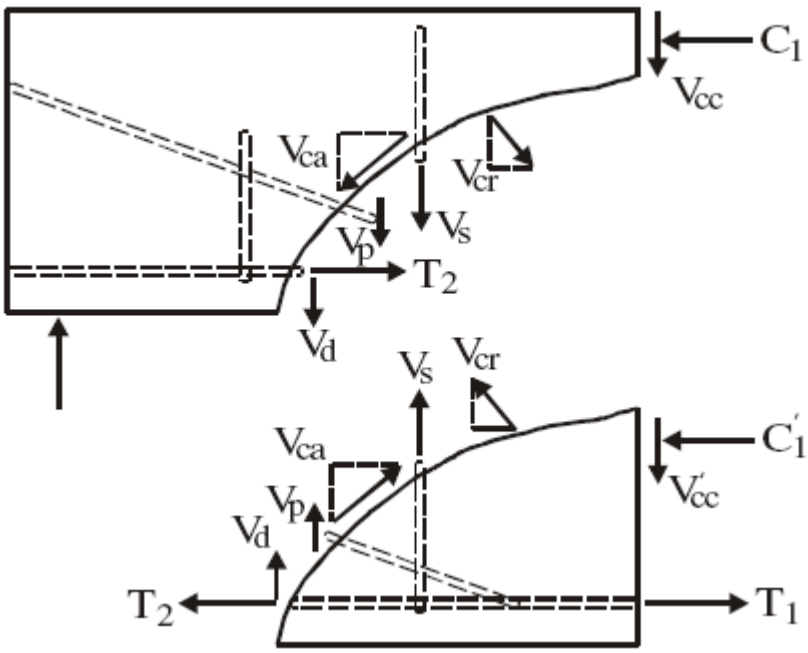

Figure 1.9. Mechanism of shear resistance (Sun and Kuchma 2007)

It is natural to assume that some shear will be carried across the uncracked compression zone. The other two, i.e. dowel action and aggregate interlock needs more explanation.

When shear displacement along an inclined crack occurs, a certain amount of shear will be transferred by the dowel action of the reinforcement because the reinforcement will try to resist this displacement. The dowel capacity depends mainly on the tensile strength of concrete. The bars will bear against the concrete cover and will crack it producing splitting along the bar in the vicinity of diagonal crack. Once the splitting cracks occur, the dowel action will loose its effectiveness. The shear carried by dowel action is about 20% of the total shear in beams without web reinforcement. Effectiveness of dowel action depends on the tensile strength of concrete, on the effective area between bars and the stiffness of the reinforcement (crack width and bar diameter).

Figure 1.10. Dowel action

The interface or surface of cracks are not smooth, the coarse aggregate particles across the crack produce roughness. When the two faces of a crack of moderate width are given, these projecting aggregate particles try to prevent the shear displacement, and thus, considerable shear can be transmitted along the crack. Measurements on test beams without web reinforcement indicated that 50 to 70% of the total shear was resisted by the aggregate interlock mechanism [3].

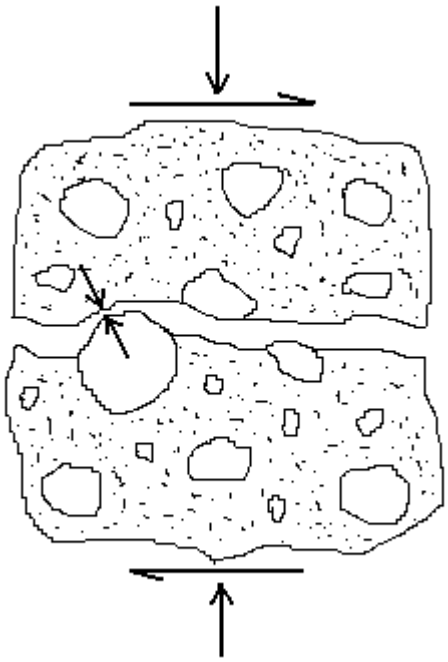

Figure 1.11. Aggregate interlock effect

1.4. Shear Design Issues of High Strength Concrete

Compared to normal strength concrete, the stress-strain curve of high strength concrete has a longer linear segment up to a higher percentage of the maximum stress, a slightly higher strain at maximum stress, and less post-peak ductility. It is generally acknowledged that the pattern of crack formation in high-strength concrete is significantly different from that seen with normal strength concrete. High strength concrete tends to be more brittle, with cracks propagating through aggregates rather than around them. The result could be a smoother fracture plane with subsequently less aggregate interlock (interface shear transfer resistance). It is also believed that, as a result, the crack related damage effect is more pronounced in higher strength concrete.

The different characteristics of high-strength concrete arouse concerns on the extension to HSC of the current shear provisions which are based on test data from specimens with normal strength concrete. Following subsections address the key issues relevant to the potential difficulties for the extension in four points, including the concrete contribution, the contribution of shear reinforcement, minimum shear reinforcement requirement and the maximum shear design stress limit.

The concrete contribution to shear resistance is principally through interface shear transfer. With the use of HSC, cracks may be smoother and the spacing between cracks may be greater due to the larger tensile strength of the concrete. These effects could reduce shear slip resistance and need to be investigated. There are other points of view which suggest that a significant portion of the load is carried by shear in the top and bottom compression zones and through dowel action. Meanwhile, other researchers contend that shear is principally a fracture process and better captured by examining the energy released with cracking as compared to that required propagating crack. These different approaches also suggest that shear capacity may not increase in proportion to the square root of the concrete compressive strength.

Codes of practice throughout the world use a parallel chord truss model for evaluating the contribution of shear reinforcement to shear resistance. The use of HSC directly impacts the importance of the accuracy of the angle, either of diagonal compression or of cracking, for evaluating the contribution of the shear reinforcement. With the use of HSC, cracks are expected to be smoother, more widely spaced and wider than for normal strength concretes. This suggests that minimum shear reinforcement requirements may need to be increased substantially for very high strength concretes. The minimum required amount of shear reinforcement is particularly important for prestressed concrete members for which large portions of their length may only contain the minimum requirement.

Maximum shear strength limit is to prevent over-reinforcement design in shear reinforcement which leads to concrete crushing prior to the stirrup yielding. For prestressing members, high strength concrete implies higher prestressing forces and flatter angles of diagonal compression than those of normal concrete members. The crushing force at the diagonal strut may occur earlier than that in normal concrete members given the same amount of vertical reinforcement. Thus with the use of high strength concrete, it is important to examine whether the maximum shear strength limit may be reduced [16].

1.5. Fibre-Reinforced Concrete

1.5.1. General

In the course of the 20th century, reinforced concrete has established itself as one of the major building materials, and today concrete structures, including buildings, bridges, power plants, dams, etc., constitute a large part of the modern civil infrastructure. Nonetheless, more efficient and industrial construction of concrete structures with improved performance can be viewed as a necessity for the future competitiveness of concrete, and is essential if the concrete construction industry is to move forward. A motive for the need of such development can be found when analyzing construction costs, which indicates that presently the expenditure on labour (e.g. preparation and dismantling of formwork, reinforcing, and casting and finishing of concrete) almost equals the cost of material. For a concrete building, roughly 40 percent of the total cost of the superstructure can be referred to labour costs. On the other hand, there are material technologies available which have the potential to significantly reduce some of the more labour-intensive construction activities. Fibre-reinforced concrete (FRC) is the major example of such materials. For instance, FRC has for a long time been perceived as a material with potential and a material which extends the versatility of concrete as a construction material, by providing an effective method of overcoming its intrinsic brittleness, and by presenting an opportunity to reduce one of the more labour-intensive activities necessary for concrete construction.

Generally, concrete containing a hydraulic cement, water, fine and coarse aggregate, and discontinuous discrete fibres is called fibre-reinforced concrete (FRC). Fibres of various shapes and sizes produced from steel, synthetics, glass, and natural materials can be used. However, for most structural and non-structural purposes, steel fibres are the most used of all fibre materials, whereas synthetic fibres are mainly used to control the early cracking in slabs. Fibres are generally added during mixing, but may also be pre-placed into a mould and the cementitious matrix subsequently infiltrated.

The constituents of a composite are generally arranged so that one or more discontinuous phases are embedded in a continuous phase. The discontinuous phase is

termed the reinforcement and the continuous phase is the matrix. In any composite material, fibres are added to improve the properties and behavior of material, and these fibres can be either continuous or discontinuous, with a preferred (e.g. uni-directional or bi-directional) or random orientation. Moreover, the matrix can be classified as either brittle or ductile; cement-based materials are typical brittle matrix materials. Depending on the characteristics of the matrix, the addition of discontinuous fibres will influence either the strength or the toughness. Normally, in a ductile matrix, short fibres are added to increase the strength, while for a brittle matrix the fibres are added primarily to improve the toughness. The main factors controlling the performance of a composite material are: the physical properties of fibres and matrix; the strength and bond between fibres and matrix; and the amount of fibres (volume fraction) and their distribution and orientation [8].

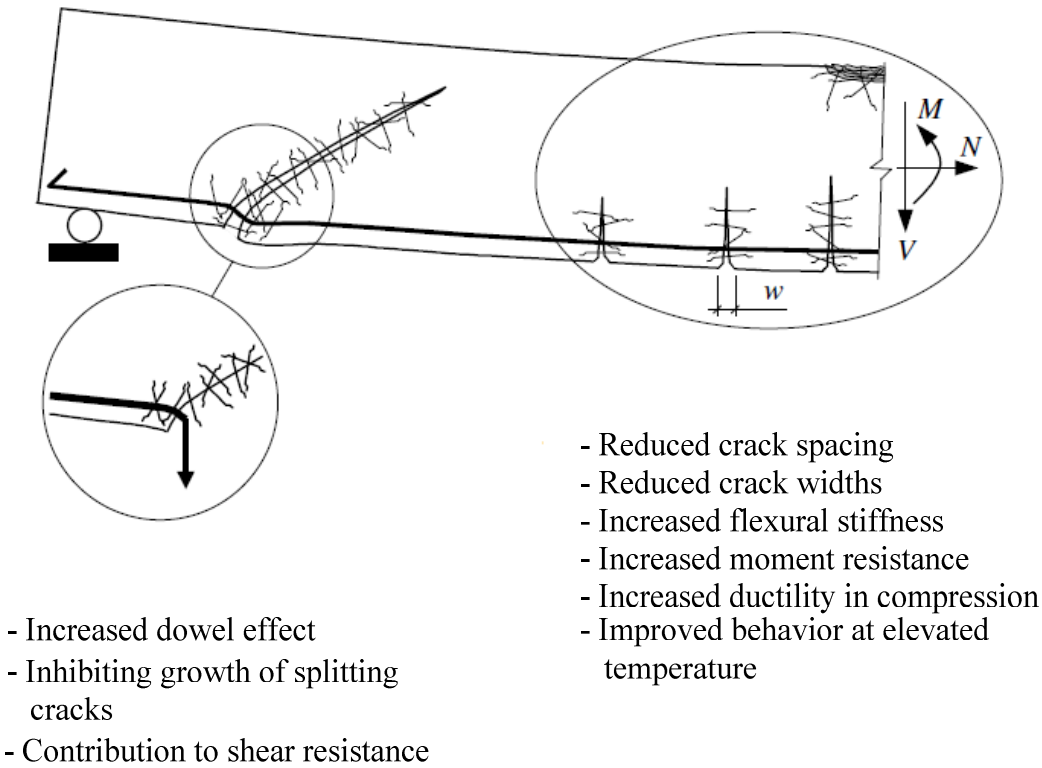

Figure 1.12. Effect of fibres on the structural behavior (Löfgren 2005)

1.5.2. Fibre Technology

There is a wide range of fibres (Figure 1.13) that can be used to improve toughness and other properties of concrete and cementitious composites. Steel fibres have been used for a considerable time, but modern steel fibres have higher slenderness and more complex geometries, and are often made of high-strength steel. Further, synthetic fibres are becoming more attractive as they can provide effective reinforcement comparable to that of steel fibres [8].

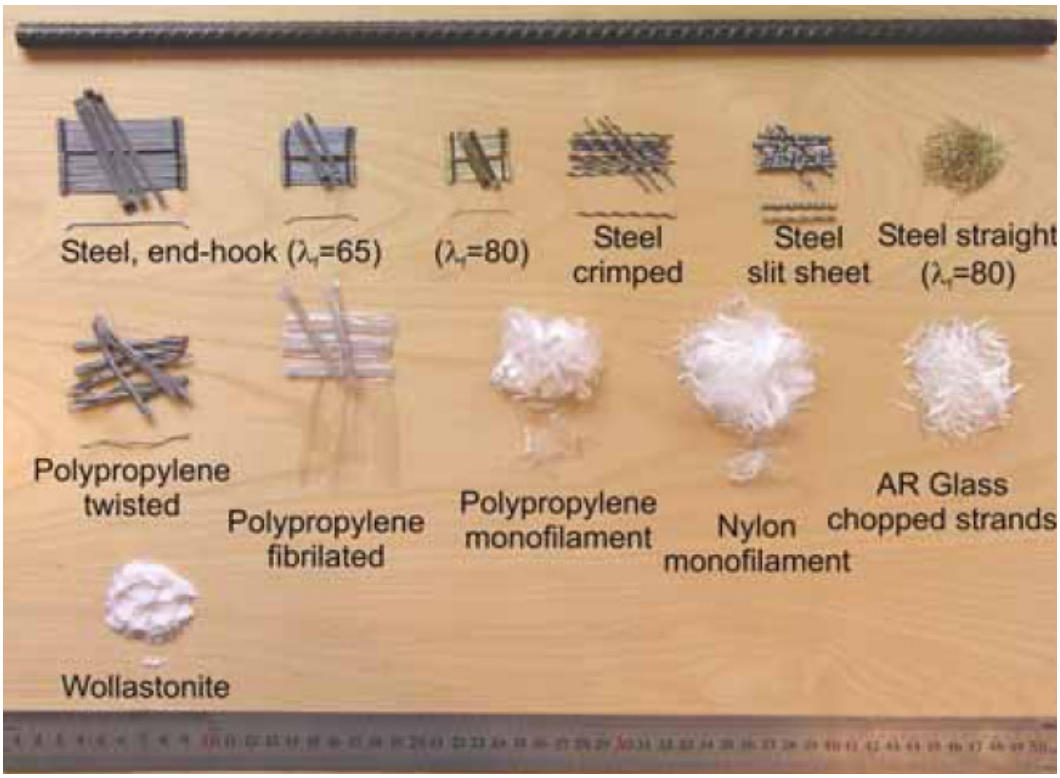

Figure 1.13. Examples of commercially available fibres (Löfgren 2005)

1.5.3. Fibre Geometries

For fibres to be effected in cementitious matrices, it has been found that they must/should have the following properties (Naaman 2003): a tensile strength significantly higher than the matrix (two to three orders of magnitude); a bond strength with the matrix preferably of the same order as, or higher, than the tensile strength of the matrix; an elastic modulus in tension significantly higher than that of the matrix (at least three times); and enough ductility so that the fibre does not fracture due to fibre abrasion or bending.

For steel fibres, usually three different variables are used for controlling the fibre performance: (1) the aspect ratio; (2) the fibre shape and surface deformation (including anchorage); and (3) surface treatment. In addition, the tensile strength of the fibre can be increased if necessary to avoid fibre fracture. The steel fibres commonly used have a round cross-section, a diameter varying from 0.2 to 1 mm, a length ranging from 10 to 60 mm, and an aspect ratio less than 100 (typically ranging from 40 to 80). Fibres often have some sort of deformation or anchorage to increase their performance [8].

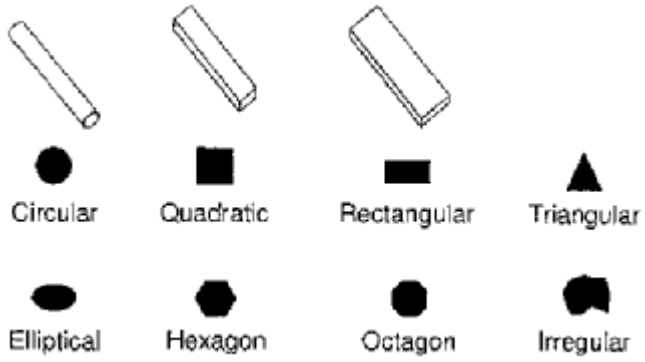

Figure 1.14. Examples of cross-sectional geometries of fibres (Löfgren 2005)

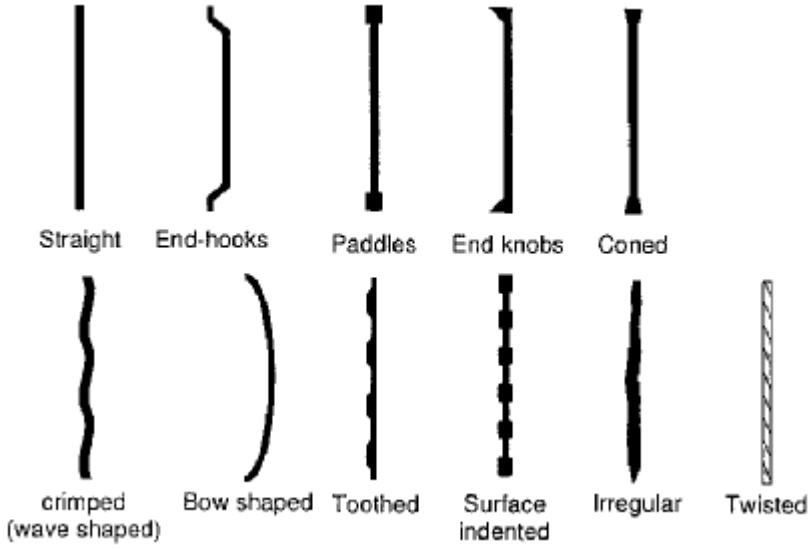

Figure 1.15. Examples of some typical fibre geometries (Löfgren 2005)

1.5.4. Fibre Materials and Physical Properties

Metallic fibres are made of either carbon steel or stainless steel and their tensile strength varies from 200 to 2,600 MPa. In the draft European Standard prEN 14889-1:2004 the following definition is provided for steel fibres: "*Steel fibres are straight or deformed pieces of cold-drawn steel wire, straight or deformed cut sheet fibres, melt extracted fibres shaved cold-drawn wire fibres and fibres milled from steel blocks which are suitable to be homogeneously mixed into concrete or mortar*". Steel fibres can also have coatings, for example of zinc for improved corrosion resistance, or brass for improved bond characteristics [8].

1.5.5. Orientation and Distribution of Fibres

The fibre orientation plays an important role for the mechanical performance of fibre-reinforced composites. The technology of dispersed reinforcement provides for direct and random (free) orientation of fibres in the concrete body [8].

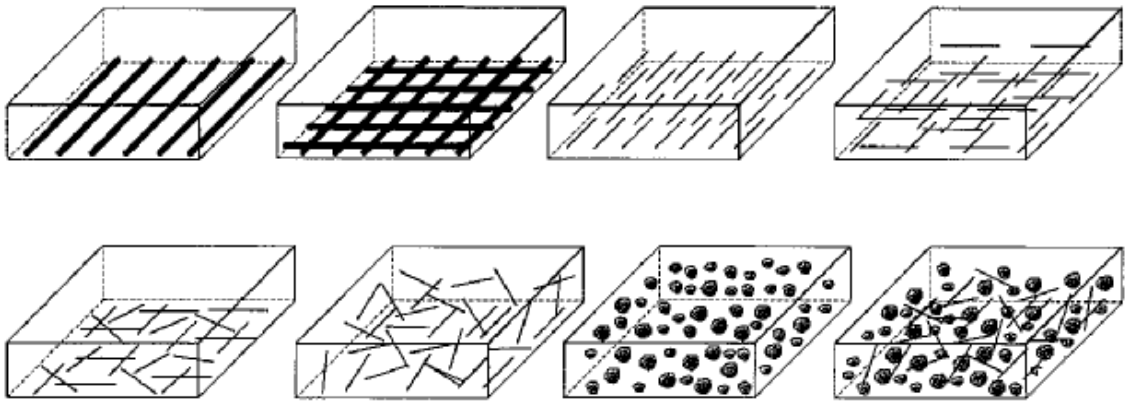

Figure 1.16. Schematic representation of different fibre composites (Löfgren 2005)

1.5.6. Mechanics of Crack Formation and Propagation

Concrete usually exhibits a large number of microcracks, especially at the interface between coarser aggregates and mortar, even before subjection to any load. These microcracks influence the mechanical behavior of concrete, and their propagation during

loading contributes to the non-linear behavior at low stress levels and causes volume expansion near failure. Many of these microcracks are caused by segregation, shrinkage or thermal expansion of the mortar. The presence of flaws and microcracks and the coalescence of these when loaded is the primary reason for the low tensile strength of concrete.

It is now generally accepted that the primary effect of fibres is that they improve the post-cracking behavior and the toughness (the resistance to fracture of concrete when stressed) rather than the tensile strength. In some of early work on fibre-reinforced concrete (Romualdi and Batson 1963), it was thought that the tensile strength could be increased due to an assumption that fibres delay the widening of microcracks (initiated at flaws) –and that the closer the fibres were spaced, the more resistance to cracking [8].

1.5.7. Shear Properties

The principle action responsible for transferring shear stresses across a crack in plain concrete is often explained as aggregate interlock and friction at the crack faces. For fibre-reinforced concrete, at low and moderate fibre dosages the cracking strength is not affected but, as soon as the matrix cracks, the fibres are activated and start to be pulled out, resulting in a significant toughening behavior (Barragán 2002). Barragán found that the maximum shear strength increased with the fibre volume fraction (for high-strength concrete the increase was significant, close to 100% with 40 kg/m3 steel fibres). For reinforced concrete, it is known that the amount of reinforcement crossing the shear plane influences the shear friction and the shear capacity due to dowel effects and a similar effect is observed for FRC. Barragán evaluated the dowel action of fibres by evaluating the residual shear stresses at different slip limits and found that this increased with the fibre volume fraction [8].

1.5.8. Flexural and Axial Forces

Deformation of tensile reinforcement is limited with 0.10% for fibre-reinforced concrete members with longitudinal reinforcement. After plastic hinge occurs, flexural strength is used for calculations, until cracks begin to be observed. At this point stresses

decrease and as a result of redistribution of loads, stresses begin to increase until a new hinge [6].

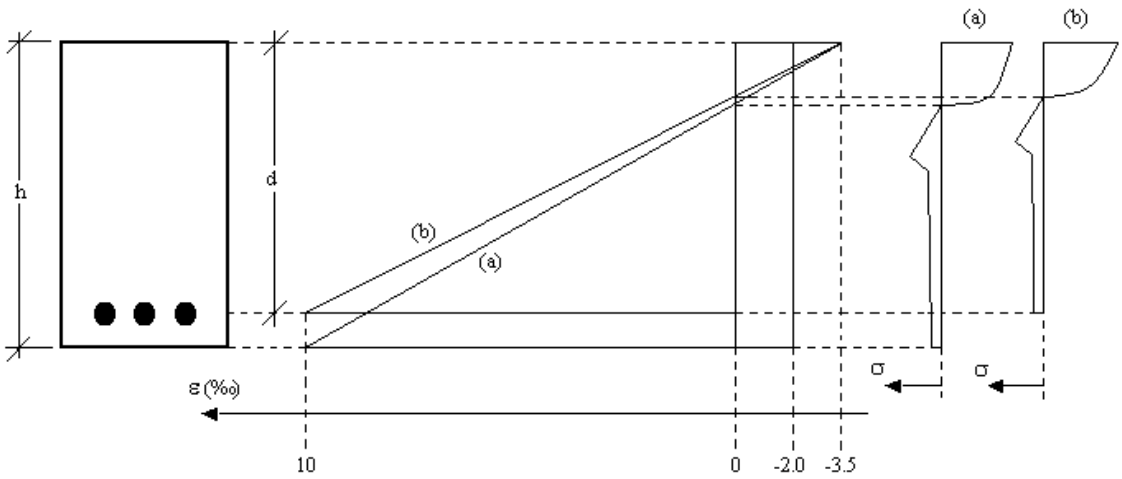

Figure 1.17. Stress and deformation (a) for concrete with fibres (b) for reinforced concrete with fibres (Dramix 2001)

1.6. Objective

The main targets of this study are listed as follows:

- to investigate the shear span-to-depth ratio effect on the shear behavior of fibre-reinforced concrete beams without web reinforcement,
- to observe the effect of the compressive strength of concrete on shear resistance,
- to examine the efficiency and effectiveness of the fibre content of concrete,
- to investigate whether fibre aspect ratio effects the shear resistance of beams.

2. LITERATURE REVIEW

2.1. Historical Background

How the concepts of diagonal tension became known as the real reason for shear failures in reinforced concrete members is not known with certainty. However, in 1899, Ritter presented the concept of diagonal tension and truss analogy with the parallel chord truss (Figure 2.1.a). The truss was composed of 45° diagonal compressive struts, the transverse tension ties, the top compression chord, and the bottom tension chord. Ritter also stated that stirrups contribute to the shear resistance of reinforced concrete by carrying tension, not shear, and proposed an equation for the design of stirrups that is very similar to the one used in current design specifications. However Ritter's viewpoints were vastly ignored in professional circles [2].

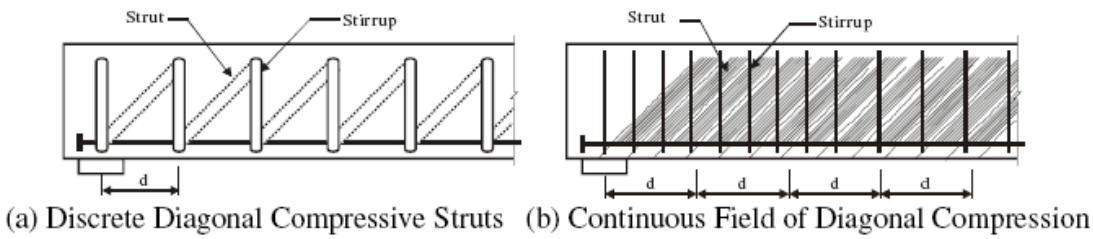

Figure 2.1. Parallel chord truss model (Sun and Kuchma 2007)

Later in 1902, Morsch further explained that rather than having discrete diagonal compressive struts there was a continuous field of diagonal compression resisting the shear as shown in (Figure 2.1.b) [16].

The debate on whether shear failures were pure shear phenomena versus tensile phenomena was finally resolved in 1906-1907 also by Morsch (1909). He pointed out that if a state of pure shear stress exists, then a tensile stress of equal magnitude must exist on a 45° plane. Therefore, since concrete is much weaker in tension than in shear or compression, tensile failure (do to the effect of shear) will occur along diagonal planes. Accordingly, Morsch presented a clear explanation of the diagonal tension mechanism, and his theory was further supported by data from von Emperger and Probst (Morsch 1909). Morsch also pointed out that a design procedure using stresses acting on diagonal planes is

difficult to establish because of the uncertainties is establishing the diagonal tension strength of the material. Therefore, an acceptable design procedure in shear for concrete structures is based on the assumption that a shear failure at the critical section occurs on an uncracked vertical plane when the applied shear stress at the section, $V_u/(b.d)$. Therefore, Morsch introduced the concept of the shear strength, $V_u/(b.d)$, as a nominal measure of diagonal tension strength.

In 1909, Talbot disputed the fact that the nominal shear strength depends only the compressive strength of concrete since diagonal tension is caused by horizontal stresses due to bending as well as stresses due to shear. Based on the results of 106 reinforced concrete beams without web reinforcement, Talbot demonstrated that the nominal shear strength depends not only on the quality of the material (thus, its strength), but also on the amount of longitudinal tensile reinforcement, the length of the beam, and the depth or stiffness of the beam. However, Talbot did not express his findings in mathematical terms, and his important concepts were forgotten.

Around 1950-1960, research and publications on the subject of shear and diagonal tension intensified dramatically as a result of a few structural failures. The research results clearly showed that shear in reinforced concrete beams is a complex phenomenon involving more than one variable. This was the in fact a return to the forgotten concepts already identified by Talbot in 1909. In the early 1950s Clark introduced a mathematical expression for the nominal shear strength prediction that included the following three variables: shear-span-to-depth ratio, the longitudinal tensile reinforcement ratio, and the compressive strength. In essence, Clark expressed Talbot's notions using a mathematical expression. The shear-span-to-depth ratio, *a/d*, was immediately recognized as an important variable since it takes into account two factors that directly affect the shear strength: the length of the beam and its depth. The main problem is using the shear-span-to-depth ratio, *a/d*, as a variable in shear stress prediction was due to the fact that the shear span, a, could only be defined for symmetrical two-point loads or for single-point loads. Research done at the University of Illinois in 1950 showed that the shear-span-to-depth ratio, *a/d,* relates the horizontal flexural stress to the diagonal tension stress and, accordingly, could be replaced by M/V (M is the bending moment and V is the shear force). It should be noted that the shear span, a, is equal to M/V for the case of simple

beams with a single point load or two symmetrical loads. Even though the two quantities are not equal for other loading conditions, the shear span, a, is often substituted with M/V in the design of reinforced concrete members. The substitution of *a/d* ratio with M/V for general loading conditions was considered to be a breakthrough in the shear design of reinforced concrete members [2].

In 1982, Mitchell and Collins proposed the compression field theory (CFT) which leads to a direct solution of crack angle. CFT is a smeared crack modeling approach that treats the cracked reinforced concrete as an orthotropic material with its own relationships. The equilibrium, compatibility, and constitutive relationships then were formulated in terms of average stresses and average strains. In CFT, the principal tensile stress in concrete is neglected with assuming that no stress is transferred across the crack. Thus, only the constitutive law for the principal compressive stress is needed.

Since the principal tensile stress in concrete is assumed to be zero, CFT overestimates deformations and gives conservative estimation of strength. To overcome these deficiencies, Vecchio and Collins (1986) proposed the modified compression field theory as a further development of CFT. Compared to CFT, modified theory takes account of the principal tensile stress and relates it to the stress transferred across the crack surface.

Since the development of the modified compression field theory, there have been three other compression field behavioral models developed, the rotating-angle softened truss model (RA-STM), introduced by Belarbi and Hsu (1995), the fixed-angle softened truss model (FA-STM) by Pang and Hsu (1996), and the disturbed stress field model (DSFM) by Vecchio (2000). Instead of checking the stress conditions at a crack as done by the modified compression field theory, both the RA-STM and the FA-STM adjust the stress-average strain relationships of the reinforcement to account for increased demand on reinforcement at the crack and bond issues between reinforcement and surrounding concrete. The DSFM is further development of the modified compression field theory where the coincident restriction of the orientation of average stress and average strain was removed by considering the influence of crack slip.

Some researchers used the crack angle rather than the angle of principal stress for evaluating the shear reinforcement contribution to shear resistance, and examined the

underlying relationships between those two sets of angles. Reineck (1990, 1991) used the angle of cracking to compute the shear capacity in his truss model with crack friction approach (TMCF). This method was implemented as a shear design procedure in the 1999 FIP Recommendations.

Tureyen and Frosh (2003) developed a shear design procedure for non-prestressing members in which the concrete contribution to shear resistance is entirely attributed to the shear in the uncracked compression zone, the interface shear transfer is neglected. Failure is assumed to occur when the principal tensile stress in the uncracked concrete above the neutral axis reaches the tensile strength of the concrete. Over the uncracked compression zone, the shear stresses distribute in a parabolic form and the normal compression stress block is in a triangular form. With using the concrete failure criterion, the shear strength of the concrete was derived assuming that a maximum shear stress and corresponding flexural stress occur at the mid-depth of the compression zone.

Compared to the evaluation of shear reinforcement contribution, there exists a wide range of opinions in the academic community to explain the concrete contribution to shear resistance at the ultimate strength of a member. These explanations range but do not limit from suggesting that V_c is entirely carried in the uncracked compression zone (Frosh, 2003), to V_c is supported by resistance to shear slip or friction along cracks (MCFT, TMCF), to V_c being calculable from fracture mechanics (Bazant and Kazemi, 1991), to V_c being sufficiently unpredictable and small as to be negligible.

Hawkins and Kuchma (2005) proposed a simplified shear design method which modifies the STD specification by reintroducing the idea of basing the concrete contribution to shear resistance on diagonal cracking strength and evaluating the contribution of shear reinforcement based on angle of diagonal cracking. This simplified method has been adopted by AASHTO LRFD Committee and will appear in the 4th Edition of the AASHTO LRFD Specifications in 2007 [16].

2.2. Previous Experimental and Numerical Research on Shear Strength of Beams

In 1995, Mays and Barnes investigated the potential for strengthening reinforced concrete members in shear. They conducted an experimental program to demonstrate the influence of shear span-to-depth ratio and beam size on the service and ultimate behavior of shear plated concrete beams. To account for the different potential types of shear failure (diagonal tension, shear compression and deep beam failure), three shear span-to-depth ratio were used (0.8, 1.8 and 4.0). In each case, they tested control beams (one without and one with conventional shear reinforcement) together with three beams strengthened with external shear plates. They observed significant increases in the shear capacity of reinforced concrete beams by bonding steel plates to both vertical faces. They indicated that this improvement in ultimate capacity reduced with the shear-span-to-depth ratio. It is also observed that the improvements in shear capacity were sensitive to beam size [4].

In 1997, Kützing investigated the shear strength of steel fibre-reinforced concrete beams and plates by using the beams loaded in 4 points with a total span of 1.54 m. He tested 3 series of beams: the NSC and the HSC beams without fibres and one NSC beam with 40 kg/m^3 of steel fibres. The longitudinal reinforcement ratio was 1.57%. The test results showed that when 40kg/m^3 of steels fibres were added to the NSC the shear capacity increased very strongly and the shear strength surpassed the ultimate bending of the test beam [5].

In 2003, Musluer examined the shear failure of high strength concrete rectangular beams without web reinforcement. He symmetrically loaded the beams with two equal concentrated loads. 6 beams with 3 different shear span-to-depth ratios (a/d = 1.20, 2.53 and 4.00) and 2 different longitudinal steel ratios (ρ= 0.93% and 1.68%) were tested to observe the shear behavior of beams. For a/d = 4.00, flexural cracks were observed for increasing loading. With further increase of loading, additional flexural cracks formed and previous cracks got longer, and then, the flexural cracks between load and support propagated towards the loading point. He specified the failure type of the beams as diagonal tension failure. When shear span-to-depth ratio was 2.53, he saw vertical flexural cracks at the beginning of loading. With increasing loads, he observed inclined cracks progressed to the load and bottom of the beam near the support and shear compression

failure occurred. The last two beams with *a/d* = 1.20 acted like an arch for the ultimate shear load. After flexural cracks occurred, diagonal cracks were observed between support and loading point. After diagonal crack, beam resisted to very high load values because the part of load was transmitted directly by diagonal compression to the support. This was not a shear transfer mechanism. It was also stated in the study that the longitudinal steel ratio influenced both the shear cracking and failure strength of beams. Results showed that the ultimate shear strength was increased 43% and the cracking shear strength increased 47% for the increasing longitudinal steel ratio from 0.93% to 1.68% [7].

In 2005, Tan and Saha made a ten-year study on steel fibre-reinforced concrete beams under sustained loads. Nine reinforced concrete beams with discrete steel fiber contents ranging from 0 to 2% were subjected to sustained flexural loading between 0.35 to 0.8 times the flexural capacity over a period of 10 years. They stated that the addition of steel fibers to concrete was effective in containing long-term deflection and restraining crack widening. They specified that steel fibers served as tensile reinforcement. It was also denoted in the study that the increase in maximum crack width could be related to the instantaneous crack width, depending on the steel fiber content [9].

In 2006, Majdzadeh, Soleimani and Banthia investigated the influence of fibres on the shear capacity of reinforced concrete beams. Both steel and synthetic fibres at variable volume fractions were investigated. Two series of tests were performed: structural tests, where RC beams were tested to failure under an applied four-point load; and materials tests, where companion fibre-reinforced concrete prisms were tested under direct shear to obtain material properties such as shear strength and shear toughness. Fibre-reinforced concrete test results indicated an almost linear increase in the shear strength of concrete with an increase in the fibre volume fraction. Fibre reinforcement enhanced the shear load capacity and shear deformation capacity of RC beams, but 1% fibre volume fraction was seen as optimal; no benefits were noted when the fibre volume fraction was increased beyond 1% [10].

In 2006, Montesinos and Gustavo constructed a database, comprising results from the tests of 147 fibre-reinforced concrete beams with deformed steel fibres and 45 companion beams without fibres. Effective beam depth, shear span-to-effective depth ratio

(*a/d*), cylinder compressive strength, fibre volume fraction, and tensile reinforcement ratio ranged from 180 to 570 mm, 1 to 6, 17.8 to 103.8 MPa, 0.25 to 2%, and 0.37 to 4.58%, respectively. They stated that their study supported the use of steel fibres as an alternative to minimum transverse shear reinforcement (stirrups or hoops) for beams. They recommended a minimum volume fraction of 0.75% as minimum shear reinforcement because all beams contained $V_f \geq 0.75\%$ exhibited a shear stress at failure greater than the conservative lower bound value [11].

In 2007, Madan, Kumar and Singh presented test data on the shear strength of a series of reinforced concrete deep beams with three steel fibre volume fractions (0, 1.0 and 1.25%), three span-to-depth ratios (0.75, 1.0 and 1.25) and three combinations of web reinforcement. They tested a total of 18 beams under two-point loading. All beams were of rectangular cross section and the effective span to overall depth ratio was varied from 1.69 to 2.5. The steel fibres used in the investigation were of diameter of 0.45mm and length of 40.5mm, straight in length having an aspect ratio of 90. During mixing balling-up of steel fibres was overcome by feeding the fibres into the mix in small quantities. It was observed that both the first crack and maximum applied load increased as the web reinforcement increased. For beams having volume fraction of fibres as 1.0% and 1.25% maximum load applied was more than for the beams containing web reinforcement. They observed no cracking in any beam up to about 50 percent of ultimate load. At about 52-60 percent of ultimate load, a diagonal tension crack formed in beams without steel fibre. Whereas in beams with steel fibres first diagonal crack formed at about 58-65 percent of the ultimate load almost in the middle of the shear span. As they increased the load, cracks propagated towards the support and loading points. They also specified that ultimate strength decreased with increasing shear span-to-depth ratio in all types of beams. Decrease in shear span reduced the occurrence and extent of flexural cracking [13].

In 2007, Shah and Ahmad made an experimental study on shear capacity of high strength concrete beams by using beams having span-to-depth ratios (*a/d*) from 3.0 to 6.0 in increments of 0.5. They tested seventy beams in two series of thirty-five beams. For each value of *a/d* ratio, five types of longitudinal steel ratios were used (ρ = 0.33, 0.73, 1.00, 1.50 and 2.00%) to determine the effect of longitudinal steel ratio. For series-I, thirty-five beams were tested without web reinforcement whereas in series-II, thirty-five beams

having shear reinforcement were used. When the load was applied and gradually increased, vertical flexural cracks occurred in the beams. With further ascending loads, inclined primary shear cracks developed in the beams. For the beams reinforced with and without web reinforcement, it was clearly observed that when the longitudinal steel increased, the shear capacity of the beams also increased for all values of *a/d* ratio. However, for the same value of longitudinal steel, the shear capacity decreased with increasing span-to-depth ratios. They specified that the longitudinal steel level maybe selected between 1% and 2% to ensure the influence of stirrups in resisting the shear failure [15].

In 2007, Bukhari and Ahmad presented a comparative analysis on shear behavior of high-strength concrete beams using various international design approaches. They tested twenty-seven high-strength beams without web reinforcement to show that the shear strength and failure mode depend on shear span-to-depth ratio (*a/d*) and longitudinal reinforcement ratio. Out of twenty-seven beams, three sets of nine beams each were cast with longitudinal steel ratio of 0.58% for Series I, 0.87% for Series II and 1.07% for Series III. The span-to-depth ratio for nine beams in each series varied from 2.0 to 6.0 in increments of 0.5. The test results demonstrated that the beams with *a/d* ratio ranging from 2.0 to 3.5 failed as result of shear crack at mid height, which propagated at the top towers the point load and at the bottom of beam and did not propagate towards the support. For *a/d* = 4.0 and 4.5, small flexural cracks occurred in the middle half of the beam. These cracks increased in number with further increase in the load and finally failure occurred as a result of flexural shear cracking. However, in beams with *a/d* greater than 4.50, flexure failure was observed. The shear strength was found to decrease with an increase in *a/d* ratio. However, for a constant value of *a/d*, the shear capacity increased with an increase in longitudinal reinforcement ratio. Comparison of test results with other approaches revealed that the experimental shear strength is more in conformity with ACI 318-02 than other design approaches for beams having tensile steel ratio higher than 1.0%. However, it was observed that the approach proposed by Zararis predicts shear capacity more effectively for the values of tensile steel ratio less than 1.0% [12].

In 2007, Salna and Marciukaitis tested 36 beams with three different shear spans (a/h = 1, 1.5 and 2) and three different fibre volumes (1, 1.5 and 2%) to examine how these factors influence the behavior of such elements. The cross-section of specimens were b =

100 mm and h = 200mm with the lengths of 500, 750 and 1000 mm. Specimens were reinforced with three volume fractions: 78.5 kg/m^3, 117.8 kg/m^3, and 157 kg/m^3 (1, 1.5 and 2%, respectively).Test results showed that plasticity, crack propagations and load capacity of elements are greatly influenced by steel fibre volume and shear span. When a/h = 1, load capacity grew from 1.62 to 1.89 times. At higher values of shear span ratio, they observed that the increase of load capacity was not very significant. For example, when a/h = 1.5 and a/h = 2, the increases were from 1.26 to 1.56 and from 1.14 to 1.54 times, respectively [14].

In 2008, Arslan proposed alternative cracking shear strength equations for slender reinforced concrete beams without stirrups. He discussed the effects of compressive strength, shear span-to-depth ratio and the percentage of longitudinal tension reinforcement ratio on the proposed cracking shear strength and ACI 318 Building Code equations. He compared the calculated and experimental results (Bresler and Scordelis 1963; Krefeld and Thurston 1966; Mphonde and Frantz 1984; Cho 2003) and observed that the proposed shear strength equations could predict cracking shear strength capacity of RC slender beams without stirrups. However, he indicated the necessity of further research to verify the proposed equations. He also stated that the experimental-to-proposed cracking shear strength ratio was not significantly influenced by increasing longitudinal reinforcement ratio, compressive strength of concrete and shear span-to-depth ratio. Finally, he specified the equivalent performance of proposed equations and ACI 318 Building Code simplified equation in the mode of cracking shear strength [18].

In 2008, Greenough and Nehdi carried out a detailed investigation on the shear behavior of fibre-reinforced self-consolidating concrete (FR-SCC) beams. They designed FR-SCC mixtures to study the influence of fibre type, fibre anchorage, and fibre content on the shear performance of reinforced concrete slender beams without stirrups, and to determine the suitability of using fibres to satisfy minimum shear reinforcement requirements. The beam specimens were 200 x 300 x 2400 mm in size with a reinforcement depth and ratio of 265 mm and 1.7%, respectively. They used two fibre materials (steel and polypropylene), three fibre types (hooked end, flat end, and wavy), and three fibre volumes (0.5, 0.75, and 1.0%). The beams were tested with an *a/d* ratio of 3 to ensure slender beam behavior. The results of tests showed that the shear capacity for the

beams with wavy fibres did not exhibit a clear trend because, at a fibre volume above 0.75%, the workability of the mixture became problematic. The steel fibre-reinforced concrete beams were able to resist larger shear loads than that of the polypropylene fibre-reinforced concrete beams for each respective fibre dosage. They also stated that all of the beams reinforced with 1.0% steel fibres resisted about 100% more load than that of the reference mixture. They noted that this improvement in shear strength corresponded approximately to that of a conventional RC beam reinforced with stirrups spaced at 250 mm. It was also observed that the steel fibre-reinforced concrete beams failed at a higher normalized stress than calculated for beams constructed with the required minimum shear reinforcement provided by stirrups, particularly for those beams with fiber volumes of 0.75 and 1.0% [19].

3. EXPERIMENTAL PROGRAM

3.1. General

Reinforced concrete has a wide usage area in the construction industry all over the world. Increased modulus of elasticity, chemical resistance, freeze thaw resistance, lower creep, lower drying shrinkage, lower permeability, and other advantages of high-strength concrete have increased its use. The calculation of stresses in concrete is difficult due to its heterogeneous nature and inclusion of reinforcement further complicates the situation. Extensive research work on shear behavior of normal as well as high-strength concrete beams has been carried out all over the world. Despite the extensive research work, shear behavior of concrete beams with normal or high strength is still controversial and needs further research. Various parameters, which affect the shear strength of reinforced concrete beams without shear reinforcement, are span-to-depth ratio (*a/d*), tensile steel ratio, aggregate type and distribution, strength of concrete, type of loading, and support conditions. In addition to this, it is well known that the use of steel fibres rises the ductility of concrete and the fracture energy. This phenomenon is transferable to the shear strength of concrete. The specimens used in tests were designed and detailed considering the effects of shear span-to-depth ratio, strength of concrete, fibre type and volume fraction.

3.2. Selection of Specimens

In order to investigate the influence of the strength of concrete, shear span-to-depth ratio, fibre type and fibre volume fraction on the shear resistance of beams without web reinforcement, twelve reinforced concrete beams were tested. 10 beams were constructed using concrete within the 28th day compressive strength range of 57 to 64 MPa (HSC). The other two had a compressive strength of 42.58 MPa (NSC).

The effect of shear span-to-depth ratio (*a/d*) on shear was observed using two span-to-depth ratios; $a/d = 2$ and 3.75. For the values that are equal or smaller than 1.5, beams behave like a tied arch. On the other hand, if *a/d* ratio has great values ($a/d > 7$), the behavior will be dominated by flexure. In order to investigate the shear behavior of beams

and observe diagonal shear cracks and shear compression failure, the shear span-to-depth ratio values of 2 and 3.75 were chosen.

Three steel fibre-volume fractions were chosen; V_f = 0, 0.5, and 0.75%. The volume fraction values bigger than 0.75% need more aggregates having a diameter smaller than 5 mm, and higher water-cement ratio. After fibre content of 0.75%, further increase in volume fraction worsens the characteristic properties of concrete due to the necessity in high proportion of fine aggregate. Therefore, the values of 0, 0.5, and 0.75% are very effective to observe the contribution of fibre content to the shear resistance of beams.

Beside the fibre-volume fraction, it was also investigated whether the type and aspect ratio of fibres influence the shear behavior of concrete. Two types of fibres with hooked ends were used; RC-80/60-BN with a length of 60 mm and diameter of 0.75 mm, and RC-65/35-BN with a length of 35 mm and diameter of 0.55 mm, which their aspect ratios are 80 and 65, respectively.

Table 3.1 illustrates the details of the test beams. All of the beams had the same cross-sectional area (125 x 250 mm) with an effective depth of 215 mm and the same longitudinal reinforcement (2ϕ16 bars). The dimensions and longitudinal reinforcement content of the beams correspond to a longitudinal reinforcement ratio of 1.5%, nearly. Two top-bars with a length of 20 cm were used at each support. The top-bars were enclosed to the flexural bars by four ϕ10 stirrups at each end to prevent the possibility of anchorage failure. No stirrups were fixed within the shear span.

Table 3.1. Summary of experimental program

Specimen	Concrete Type	Longitudinal Reinforcement Ratio (ρ)	Volume Fraction (V_f,%)	Fibre Type	Aspect Ratio of Fibre (L/D)	f_{ck} (MPa)	a/d
BEAM-01	HSC	2ϕ16 - 1.5%	0.00	-	-	57.57	2.00
BEAM-02	HSC	2ϕ16 - 1.5%	0.00	-	-	57.57	3.75
BEAM-03	HSC	2ϕ16 - 1.5%	0.50	RC-65/35-BN	35/0.55 = 65	60.16	2.00
BEAM-04	HSC	2ϕ16 - 1.5%	0.50	RC-65/35-BN	35/0.55 = 65	60.16	3.75
BEAM-05	HSC	2ϕ16 - 1.5%	0.75	RC-65/35-BN	35/0.55 = 65	61.68	2.00
BEAM-06	HSC	2ϕ16 - 1.5%	0.75	RC-65/35-BN	35/0.55 = 65	61.68	3.75
BEAM-07	HSC	2ϕ16 - 1.5%	0.50	RC-80/60-BN	60/0.75 = 80	60.86	2.00
BEAM-08	HSC	2ϕ16 - 1.5%	0.50	RC-80/60-BN	60/0.75 = 80	60.86	3.75
BEAM-09	HSC	2ϕ16 - 1.5%	0.75	RC-80/60-BN	60/0.75 = 80	63.59	2.00
BEAM-10	HSC	2ϕ16 - 1.5%	0.75	RC-80/60-BN	60/0.75 = 80	63.59	3.75
BEAM-11	NSC	2ϕ16 - 1.5%	0.00	-	-	42.58	2.00
BEAM-12	NSC	2ϕ16 - 1.5%	0.00	-	-	42.58	3.75

3.3. Material Properties

3.3.1. Concrete Mixture Designs

Concrete mix was prepared in the laboratory of Öz-Seç Concrete Plant in Hadımköy. Two types of concrete mix were designed to observe the effect of the compressive strength of concrete on shear resisting mechanism. Small W/C value was used to produce high strength concrete (HSC), and high value for the normal strength concrete (NSC). The mix design values for the two types of concrete are shown in Table 3.2 and Table 3.3. In order to determine the compressive strength of concrete in accordance with TS-500 [17], cylinder samples with a diameter of 150 mm and height of 300 mm were used (Figure 3.2 and Figure 3.3). Sulfur capping on each cylinder was made before compression tests, for proper stress distribution. It was observed that the fibre-reinforced concrete samples did not disintegrate after ultimate load was reached, whereas samples without fibres crushed.

Table 3.2. High strength concrete mix design

HSC	
Material	Weight for m^3 (kg/m^3)
Cement (PKC/B 42.5-R)	605
Water	169.5
Sand (0-4mm)	260
Fine Aggregate (0-5mm)	528
No1 Aggregate (4-11.2mm)	865
Sika Visco-create SF12	8.34
Total Weight (kg)	2435.84
W/C	28%
Slump (cm)	10.6

Table 3.3. Normal strength concrete mix design

NSC	
Material	Weight for m^3 (kg/m^3)
Cement (PKC/B 42.5-R)	315
Water	165
Sand (0-4mm)	250
Fine Aggregate (0-5mm)	530
No1 Aggregate (4-11.2mm)	540
No2 Aggregate (11.2-22.4mm)	540
Sika Visco-create RMC-310W	3.78
Total Weight (kg)	2348.28
W/C	54%
Slump (cm)	13.8

Figure 3.1. Production of Beams

Figure 3.2. Compression Testing Machine

Figure 3.3. Cylinder Samples

3.3.2. Reinforcing Steel

ϕ16 ribbed bars with a characteristic yield strength of 420 MPa were used for the longitudinal reinforcement. Also ribbed bars with a diameter of 10 mm were used as stirrups.

3.3.3. Steel Fibres

Two types of fibres were added to concrete mix. The first type, RC-80/60-BN is a cold-drawn wire fibre, with hooked ends, has a length of 60 mm and diameter of 0.75 mm (aspect ratio equals to 80). The second one, RC-65/35-BN also has hooked ends. 65 indicates the aspect ratio of fibres. The length and diameter of fibres are 35 and 0.55 mm, respectively. The characteristic properties of the two types of fibres and recommended maximum dosage are given in Table 3.4 and Table 3.5, respectively. Concrete was partially poured from trans-mixer to a concrete mixer to provide the proper volume fraction. Fibres were mixed with concrete in a random orientation.

Table 3.4. Characteristic properties of RC-80/60-BN and RC-65/35-BN

Fibre Type	Length (mm)	Diameter (mm)	Aspect Ratio (L/D)	Min. Tensile Strength (MPa)	Fibres / kg
RC-80/60-BN	60	0.75	80	1,050	4,600
RC-65/35-BN	35	0.55	65	1,100	14,500

Table 3.5. Maximum fibre dosages

Fibre Type	Maximum aggregate size (mm)	Maximum Dosage (kg/m^3)	
		pour	pump
RC-80/60-BN	8	60	45
	16	50	35
	32	35	30
RC-65/35-BN	8	110	80
	16	70	55
	32	60	45

3.4. Test Set-up and Instrumentation

The specimens were tested in Bogazici University Structures Laboratory. The beams were supported by a hinge on one end and a roller at the other as shown in Figure 3.4, to prevent developing significant axial forces that could cause strut action. Two equal loads were symmetrically applied to the beams using steel profiles and two 80 mm-wide loading plates. The loading capacity was 200 kN. The increment in load and mid-span displacement were recorded for each second. A strain gauge was used to measure the mid-span displacement. In order to observe cracks accurately, the beams were painted to white before testing. The first cracking load of each beam was noted and crack propagation was showed by red lines and marked with the same number for the same load.

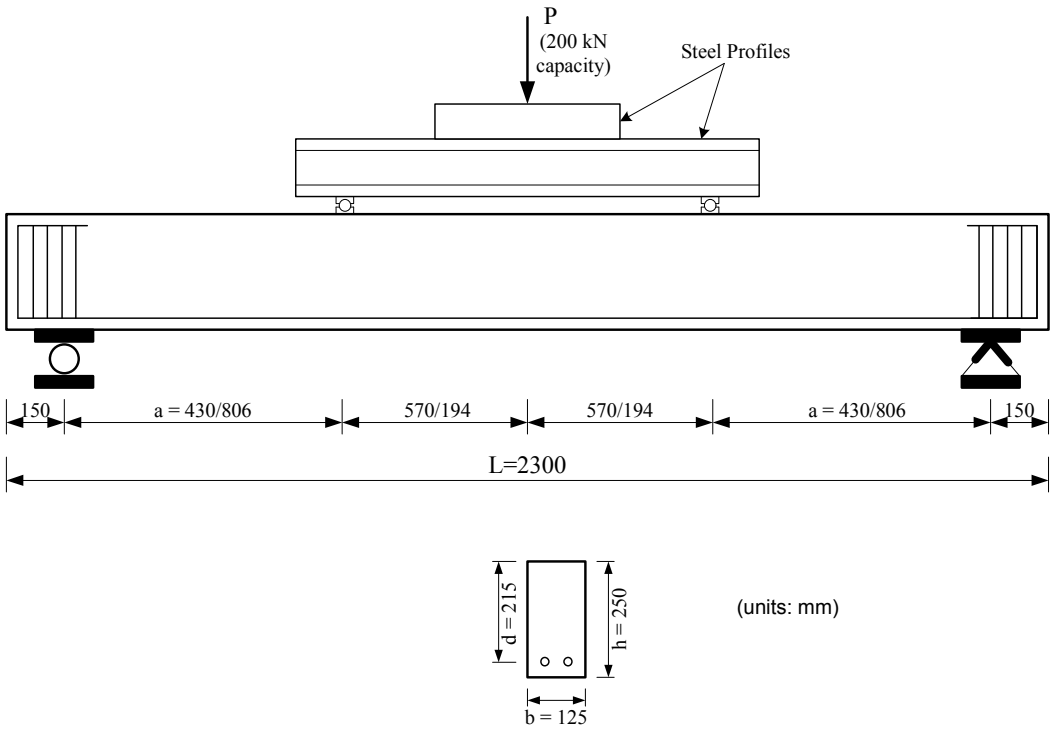

Figure 3.4. Test set-up

Figure 3.5. Test set-up in the Laboratory

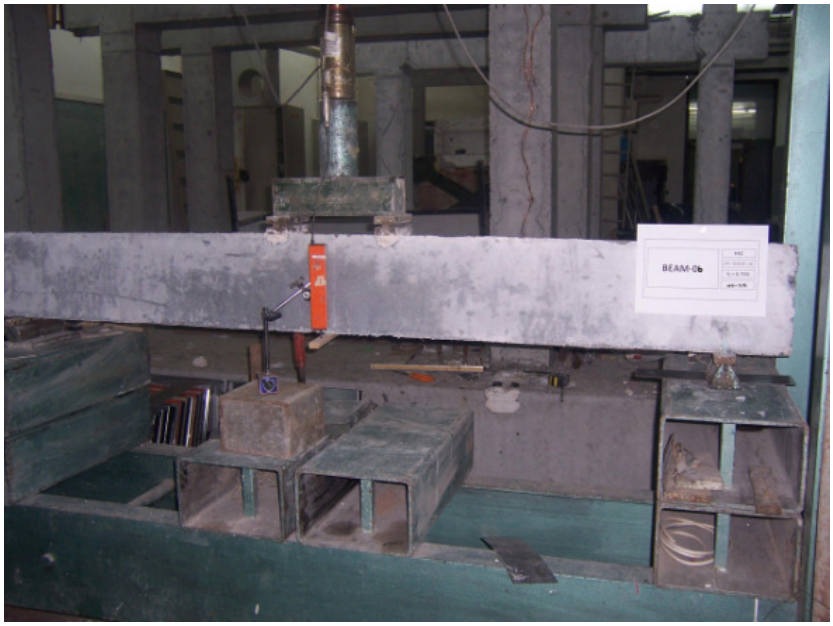

Figure 3.6. Test set-up and instrumentation

4. TEST RESULTS

4.1. General

In this chapter, test observations are presented to characterize the shear behavior of the fibre-reinforced concrete beam specimens. Observations noted during the experiments are given with the related photographs of the damaged beams. In addition, for each beam, load-time and load-displacement diagrams are also presented.

4.2. Observations on the Specimens

4.2.1. Specimen BEAM-01

At early stages of loading, vertical flexural cracks formed. As the load was increased, cracks in the shear span began to get inclined and previous flexural cracks elongated. With further increase of load, the inclined crack progressed to the point of load application and support of the beam. At this stage, a diagonal crack was fully developed. The beam continued to carry the increasing load with fully developed diagonal cracks. Finally, shear compression failure occurred by crushing of concrete below the load application point (Figures 4.1 and 4.2). The change in load with time and the load-displacement relationship for the specimen BEAM-01 are given in figures 4.3 and 4.4, respectively.

The cracking and maximum shear stresses were 0.96 (V_{cr} / $b_w d$) and 2.56 (V_u / $b_w d$) MPa, respectively. The maximum displacement recorded was 12.40 mm.

Figure 4.1. Crack propagation and damaged shape of the specimen BEAM-01

Figure 4.2. Damaged shape of the specimen BEAM-01

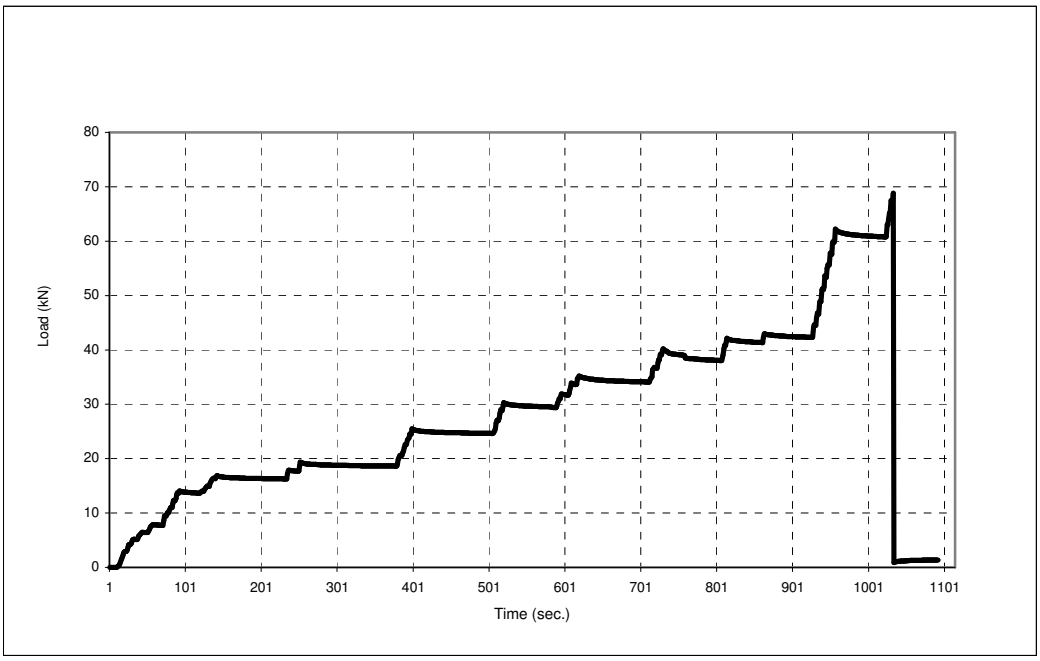

Figure 4.3. Change in load with time (BEAM-01)

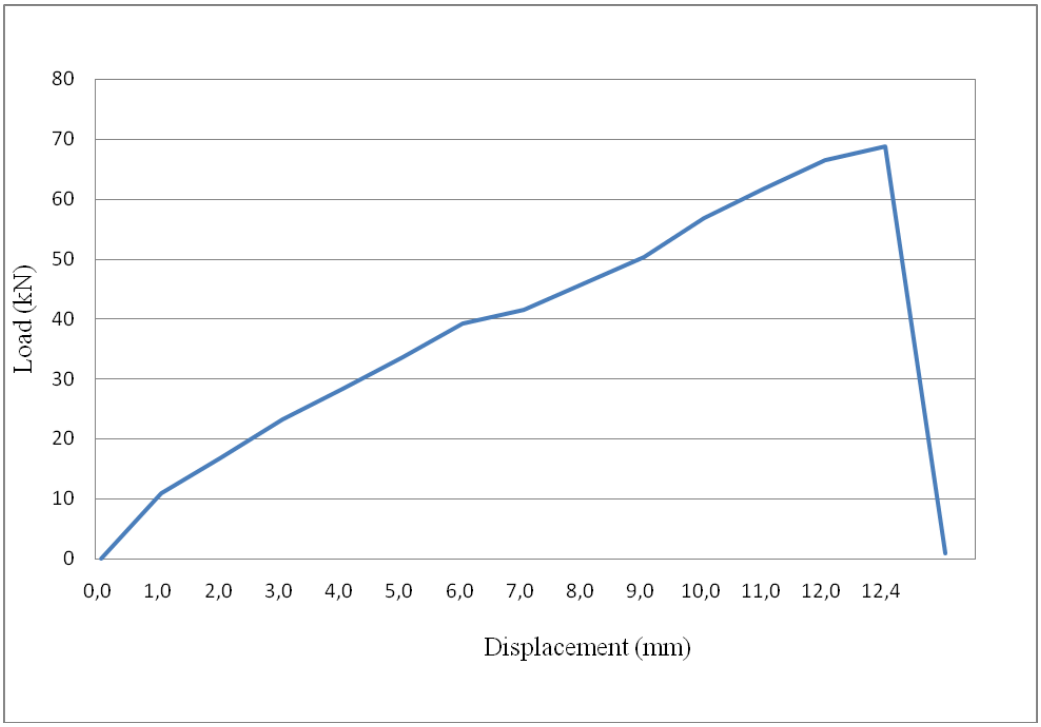

Figure 4.4. Load-displacement relationship for BEAM-01

4.2.2. Specimen BEAM-02

For specimen BEAM-02, flexural cracks first appeared in the maximum moment region. With the increase of load, flexural cracks progressed vertically and new almost vertical cracks formed in the shear span. As the load was increased, some of the flexural cracks in the shear span were inclined towards the load application point as they progressed upwards. With further increase in load, the inclined cracks began to progress downward to the level of longitudinal steel. Finally, the beam failed suddenly along the diagonal crack (Figures 4.5 and 4.6). The maximum stress carried by the beam was 1.27 MPa. The maximum displacement before the beam failed by diagonal tension was 6.62 mm.

Figure 4.5. Crack propagation and damaged shape of the specimen BEAM-02

Figure 4.6. Damaged shape of the specimen BEAM-02

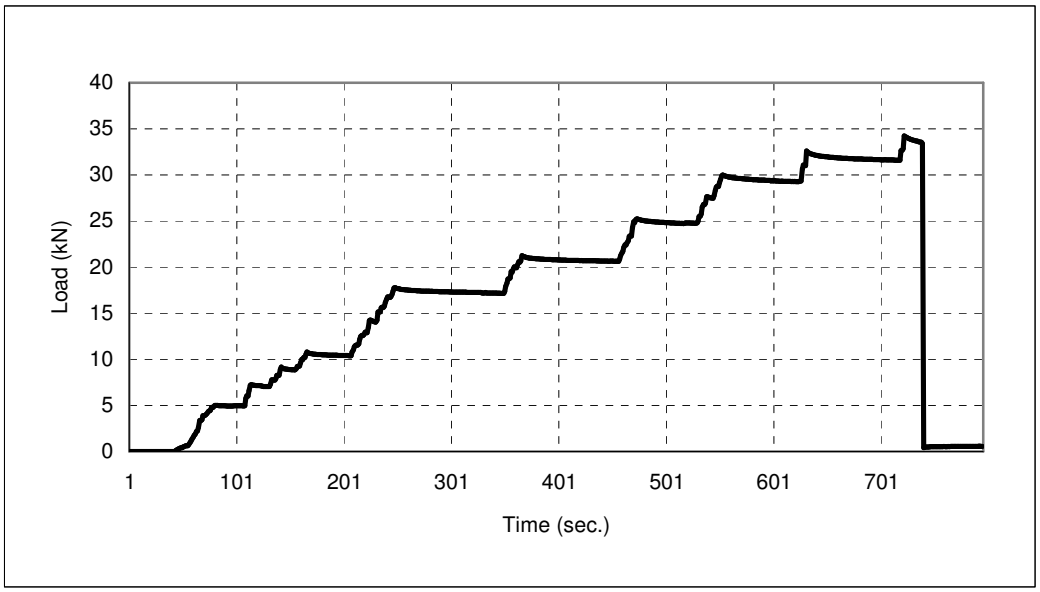

Figure 4.7. Change in load with time (BEAM-02)

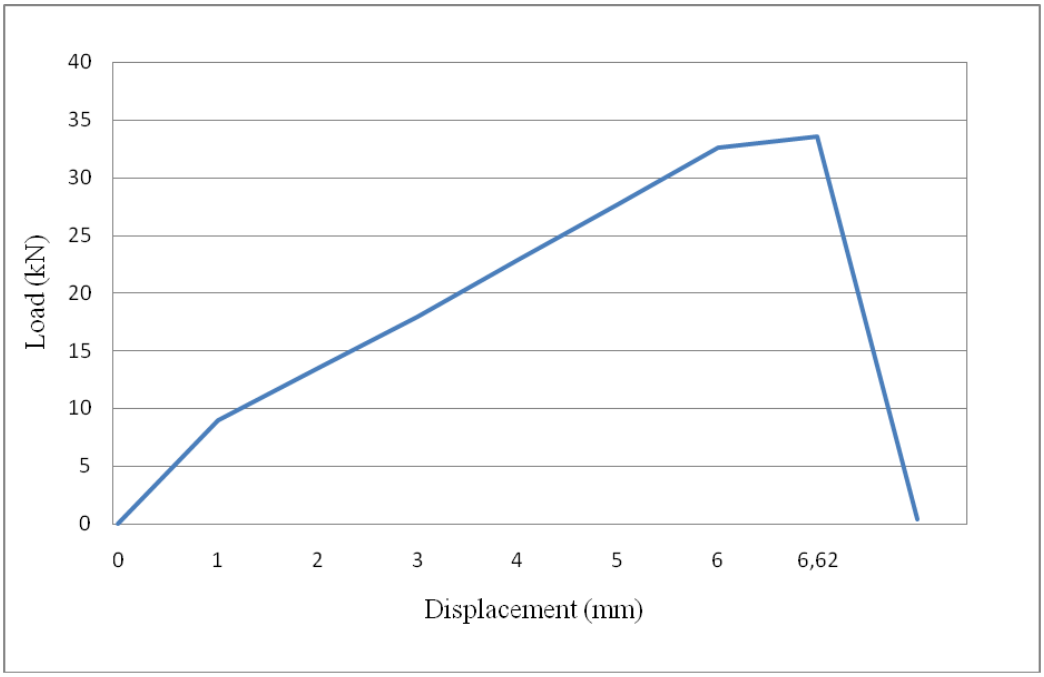

Figure 4.8. Load-displacement relationship for BEAM-02

4.2.3. Specimen BEAM-03

Similar to the specimen BEAM-01, specimen BEAM-03 failed under shear compression (Figures 4.9 and 4.10). Due to the influence of fibres, cracking stress and the ultimate shear stress at failure increased. The cracking stress, maximum shear stress and maximum displacement were 1.15, 2.73 MPa, and 12.80 mm, respectively.

Figure 4.9. Crack propagation and damaged shape of the specimen BEAM-03

Figure 4.10. Damaged shape of the specimen BEAM-03

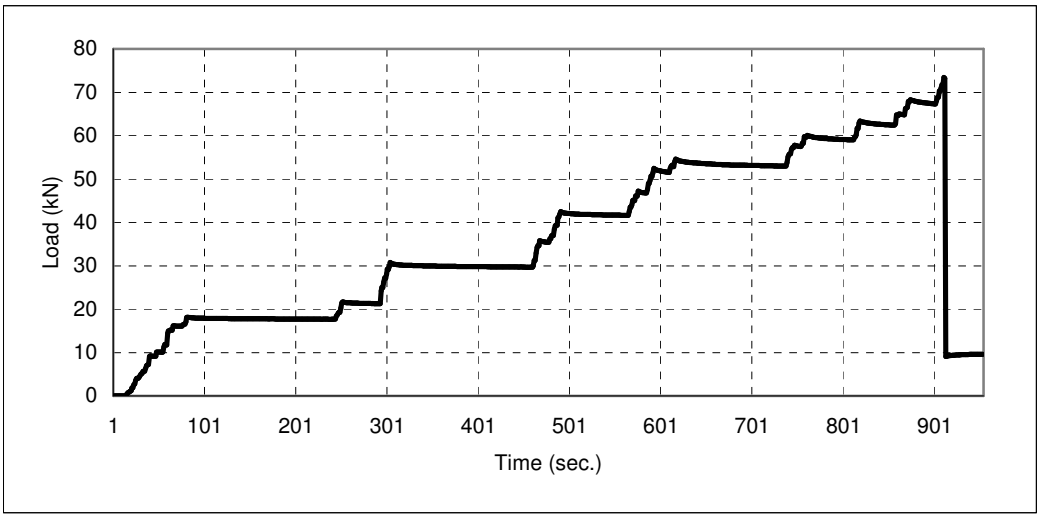

Figure 4.11. Change in load with time (BEAM-03)

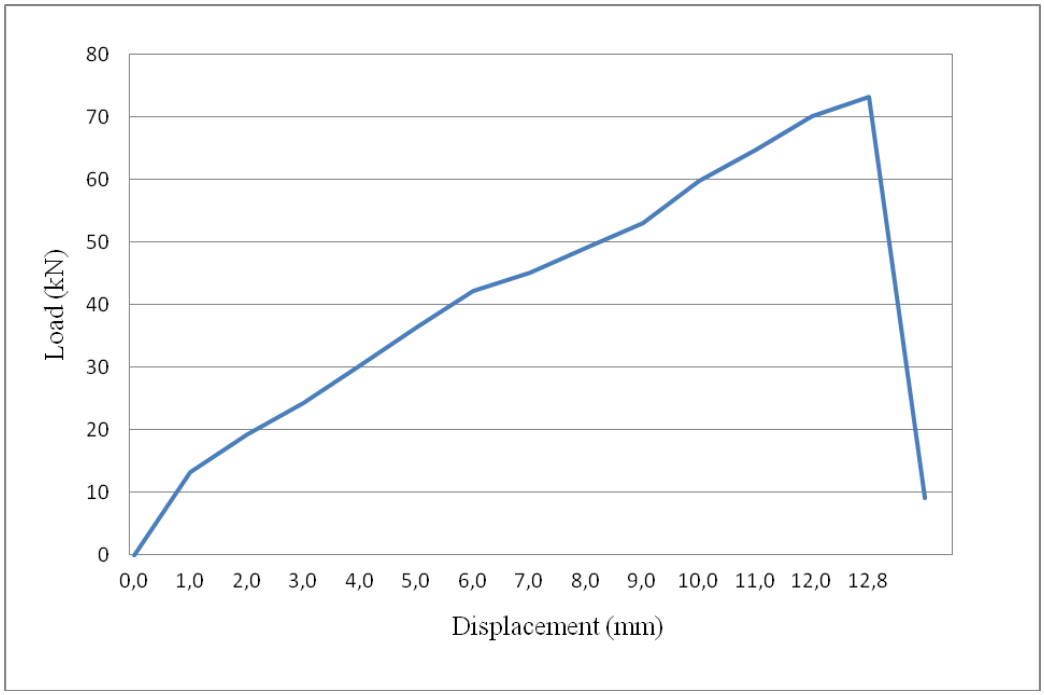

Figure 4.12. Load-displacement relationship for BEAM-03

4.2.4. Specimen BEAM-04

After initial development of flexural cracks, flexural cracks propagated vertically and new cracks were observed in the shear span. As the load was increased, some of the flexural cracks in the shear span were inclined towards the load application point similar to the specimen BEAM-02. The cracking stress was 0.97 MPa. A brittle and sudden diagonal tension failure occurred, finally (Figures 4.13 and 4.14). The maximum stress carried by the beam was 1.56 MPa. It was observed that the 0.5% fibre content increased the shear carrying capacity of the beam. The maximum displacement was recorded as 10.38 mm. The change in load with time and the load-displacement relationship for the specimen BEAM-01 are given in figures 4.13 and 4.14, respectively.

Figure 4.13. Crack propagation and damaged shape of the specimen BEAM-04

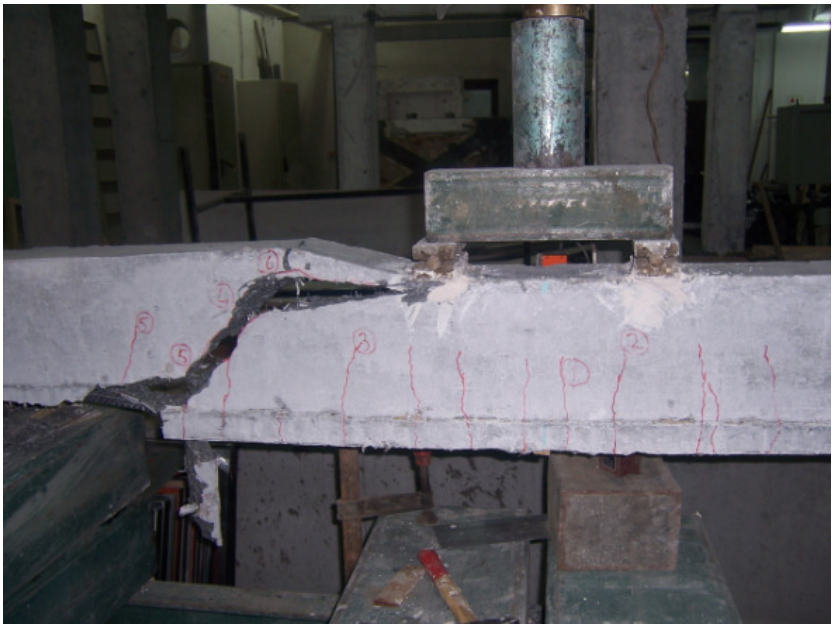

Figure 4.14. Damaged shape of the specimen BEAM-04

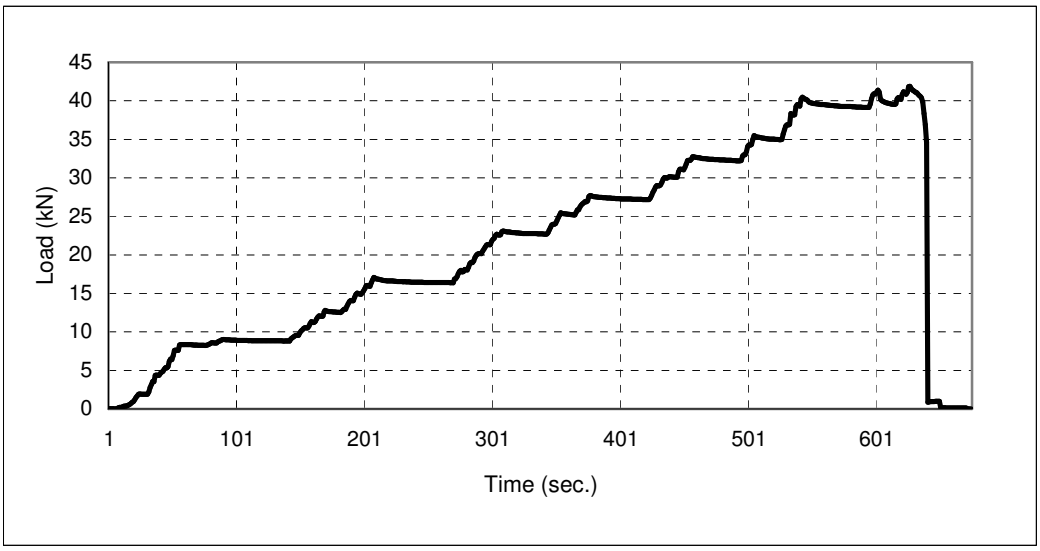

Figure 4.15. Change in load with time (BEAM-04)

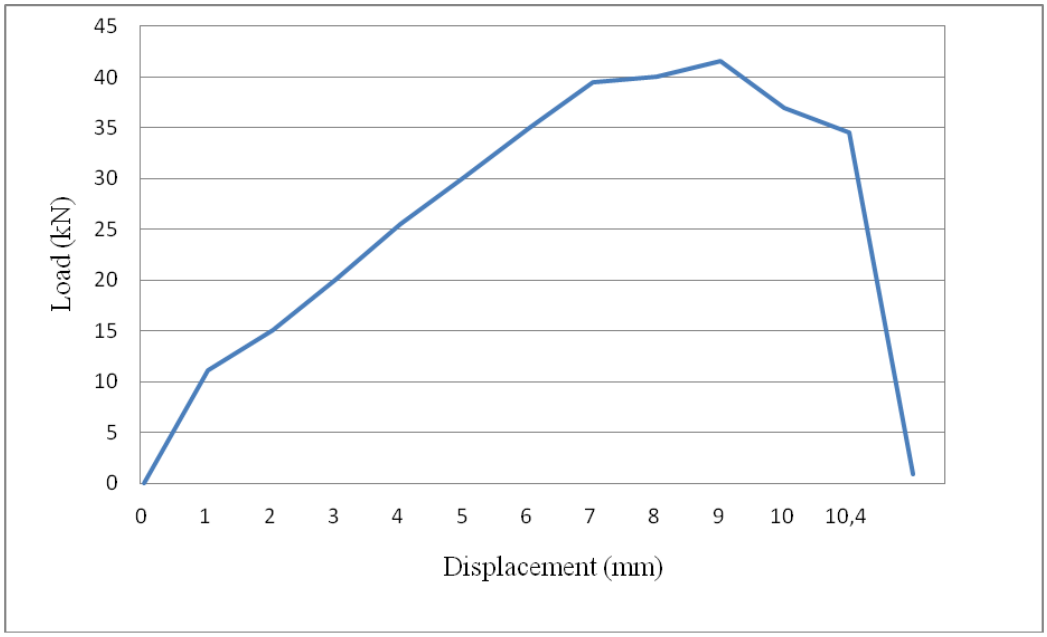

Figure 4.16. Load-displacement relationship for BEAM-04

4.2.5. Specimen BEAM-05

Similar to the specimens BEAM-01 and BEAM-03, for specimen BEAM-05, after development of the initial flexural and inclined cracks, the beam continued to carry the increasing load, with fully-developed diagonal cracks, and then, the beam failed by shear compression (Figures 4.17 and 4.18). The maximum average shear stress was larger than both the shear stresses for the specimens BEAM-01 and BEAM-03: 2.94 MPa. The

increase in fibre volume fraction from 0.5% to 0.75% increased the shear carrying capacity of the beam, significantly. The cracking stress and maximum displacement were observed as 1.32 MPa and 13.28 mm, respectively.

Figure 4.17. Crack propagation and damaged shape of the specimen BEAM-05

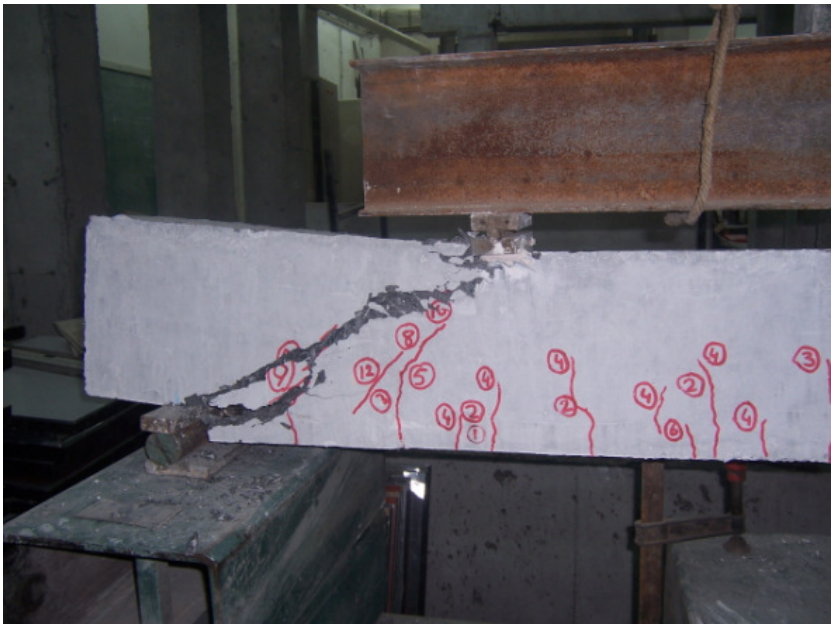

Figure 4.18. Damaged shape of the specimen BEAM-05

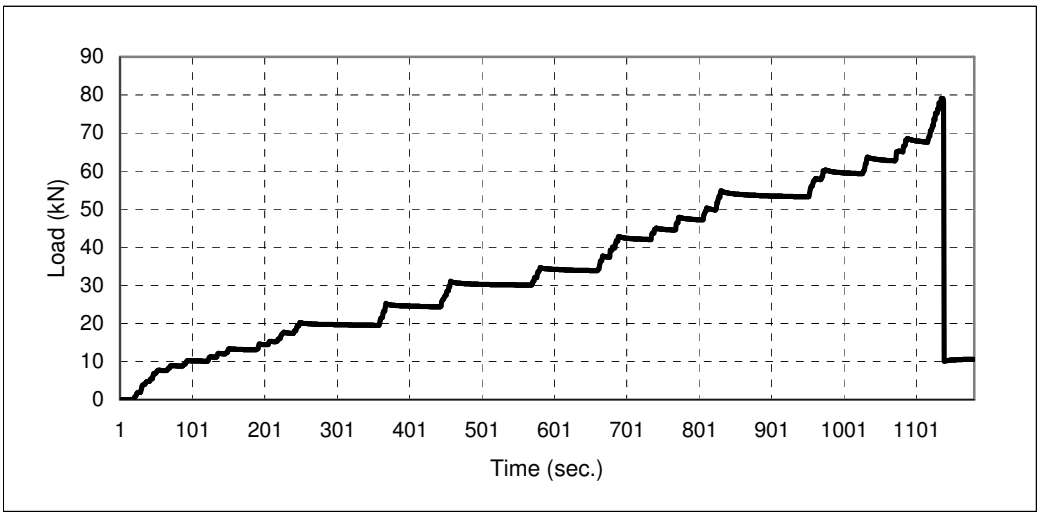

Figure 4.19. Change in load with time (BEAM-05)

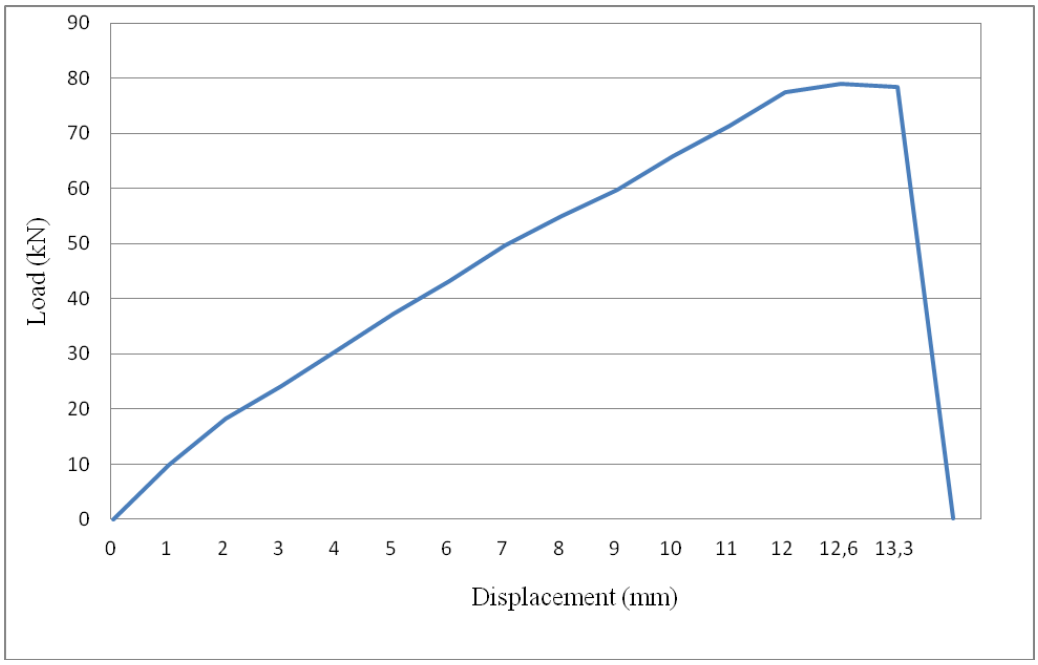

Figure 4.20. Load-displacement relationship for BEAM-05

4.2.6. Specimen BEAM-06

Although the shear span-to-depth ratio of specimen BEAM-06 was 3.75, the beam behaved as if the shear span-to-depth ratio was larger than 7 and failed in flexure by yielding of the longitudinal reinforcement and then crushing of concrete in the compression zone. Although the flexural cracks within the shear span were slightly inclined, no diagonal cracks formed. After a certain point, the beam did not carry

additional load with increasing displacement due to yielding of longitudinal reinforcement. The crack widths of the flexural cracks extremely increased at the zone of the maximum moment. Finally, a flexural failure took place by crushing of concrete in compression zone. A very high displacement value was observed after failure: 60.50 mm (Figure 4.23). The cracking and ultimate shear stresses were 1.09 and 1.74 MPa. It can be considered that 0.75% fibre content behaved like confinement and caused an increase in the shear carrying capacity and displacement ability of the beam.

Figure 4.21. Crack propagation and damaged shape of the specimen BEAM-06

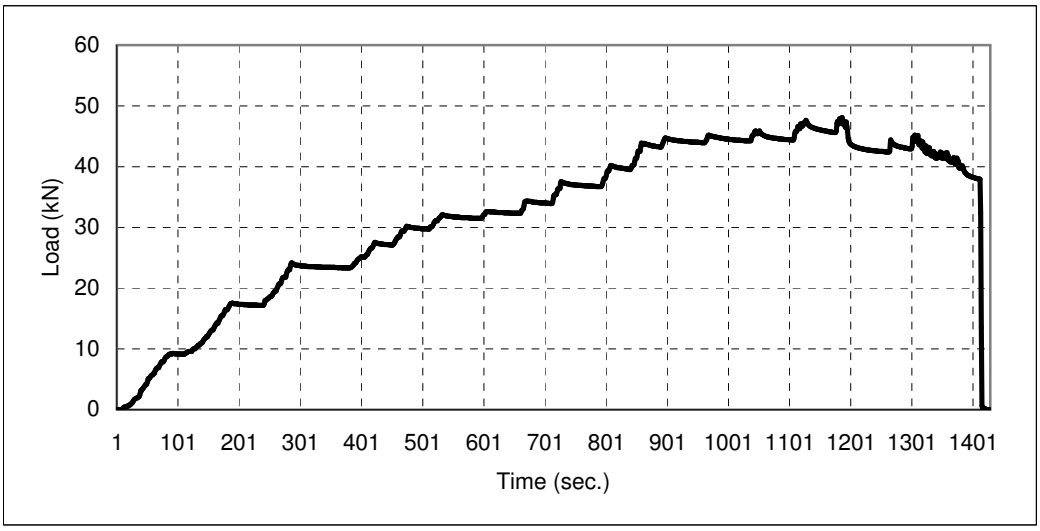

Figure 4.22. Change in load with time (BEAM-06)

Figure 4.23. Load-displacement relationship for BEAM-06

4.2.7. Specimen BEAM-07

The specimen BEAM-07 failed under shear. With the same volume fraction, the value of V_u / $b_w d$ was larger than the V_u / $b_w d$ value of the specimen reinforced by the fibres with an aspect ratio of 65 (RC-65/35-BN fibres). The ultimate stress was 2.94 MPa while the maximum stress of the specimen BEAM-03 was 2.73 MPa. The cracking stress and ultimate displacement were 1.24 MPa and 13.40 mm.

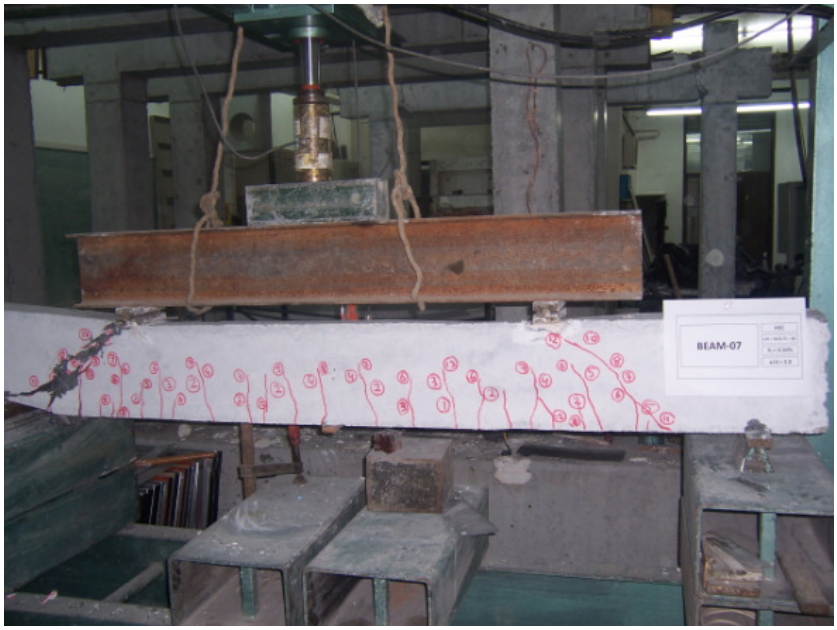

Figure 4.24. Crack propagation and damaged shape of the specimen BEAM-07

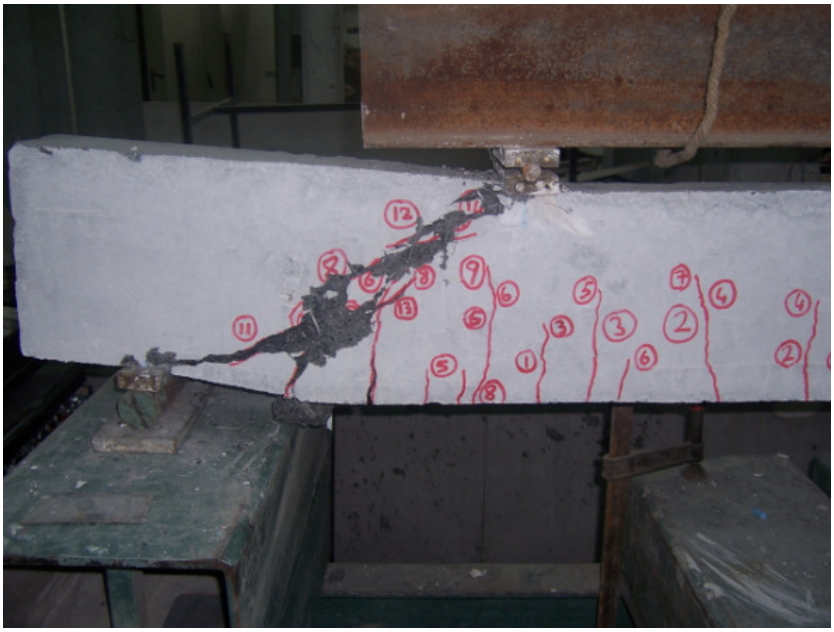

Figure 4.25. Damaged shape of the specimen BEAM-07

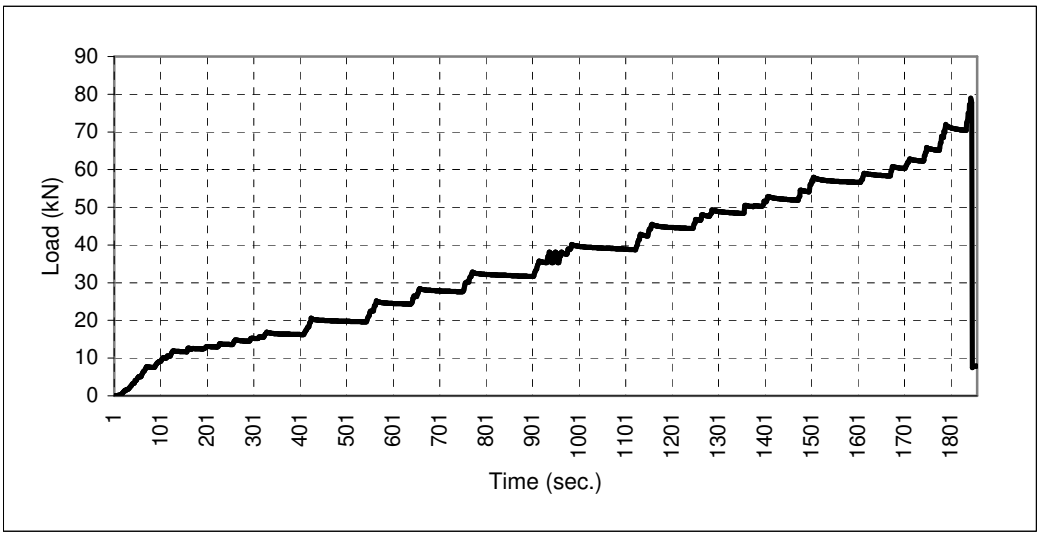

Figure 4.26. Change in load with time (BEAM-07)

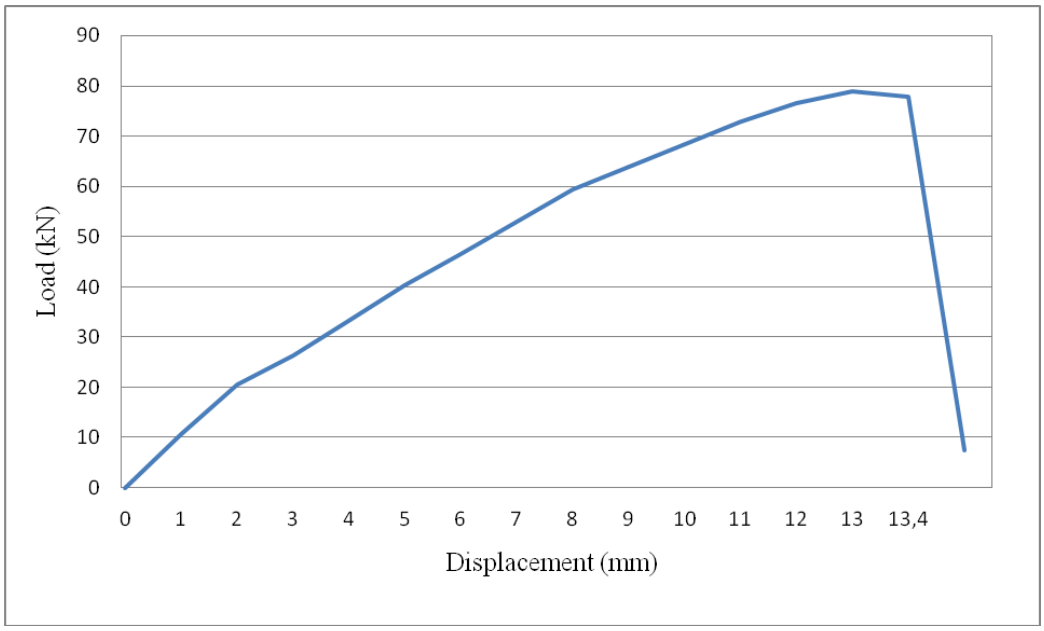

Figure 4.27. Load-displacement relationship for BEAM-07

4.2.8. Specimen BEAM-08

For the same shear span-to-depth ratio, the ultimate load was larger than both the maximum loads of the specimen without fibres and specimen with a volume fraction of 0.5% and short fibres. Diagonal tension failure occurred (Figures 4.28 and 4.29) with an ultimate shear stress (V_u / b_wd) of 1.39 MPa. The cracking stress (V_{cr} / b_wd) and maximum deflection were 0.89 MPa and 12.80 mm.

Figure 4.28. Crack propagation and damaged shape of the specimen BEAM-08

Figure 4.29. Damaged shape of the specimen BEAM-08

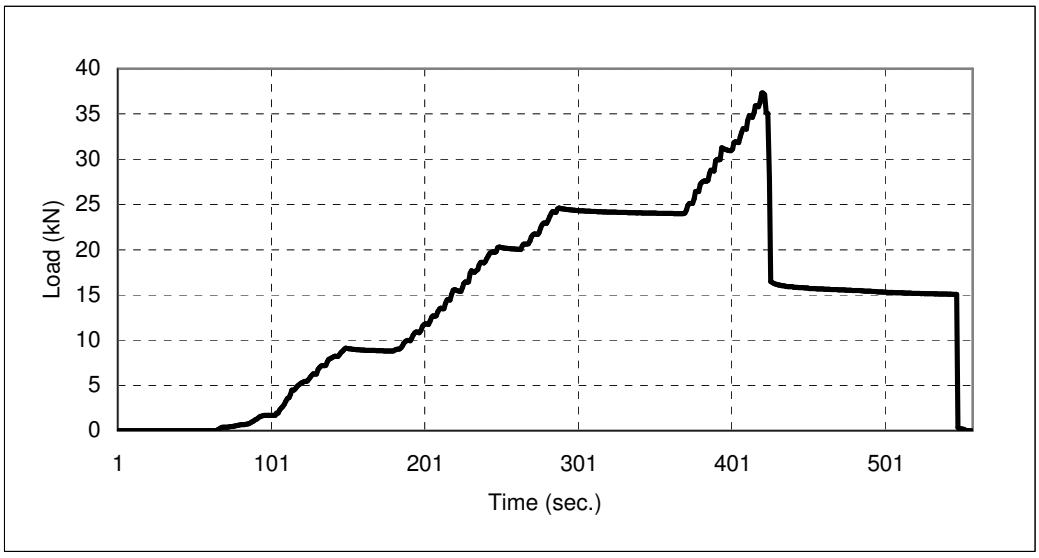

Figure 4.30. Change in load with time (BEAM-08)

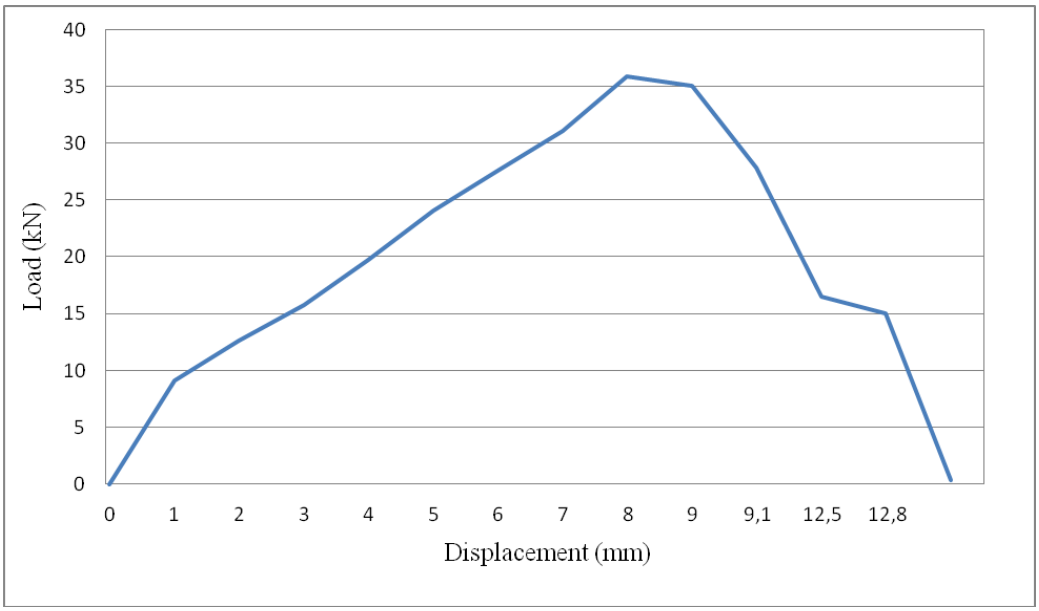

Figure 4.31. Load-displacement relationship for BEAM-08

4.2.9. Specimen BEAM-09

After initial development of flexural cracks, with further increase in load, some of these flexural cracks in shear span began to get inclined. As the load was increased, a diagonal crack formed. With further increase in load, the width of this diagonal crack increased. It was expected that failure took place by shear compression. However, after a point, the width of the diagonal crack began to decrease due to the influence of aggregate

interlock and well-orientation of fibres along the crack (well-distributed fibres perpendicular to the crack). Redistribution took place and the stress in shear zone began to expand towards the mid-span of the specimen BEAM-09. Finally, failure occurred by crushing of concrete in compression zone (Figures 4.33 and 4.34). This can be explained as the beam was confined by long fibres with a volume fraction of 0.75%. For the shear span-to-depth ratio of 2, the specimen BEAM-05 having fibres with an aspect ratio of 65 did not provide this effect. The specimen reached a very high level of deflection: 57.34 mm. The average cracking and ultimate stresses were 1.54 and 3.38 MPa. These values were the highest ones recorded. It can be concluded that RC-80/60-BN fibres with a volume fraction of 0.75% can be used as an alternative confinement technology. The results of the specimen BEAM-10 verify this proposal.

Figure 4.32. Crack propagation on the specimen BEAM-09

Figure 4.33. Crack propagation and damaged shape of the specimen BEAM-09

Figure 4.34. Damaged shape of the specimen BEAM-09

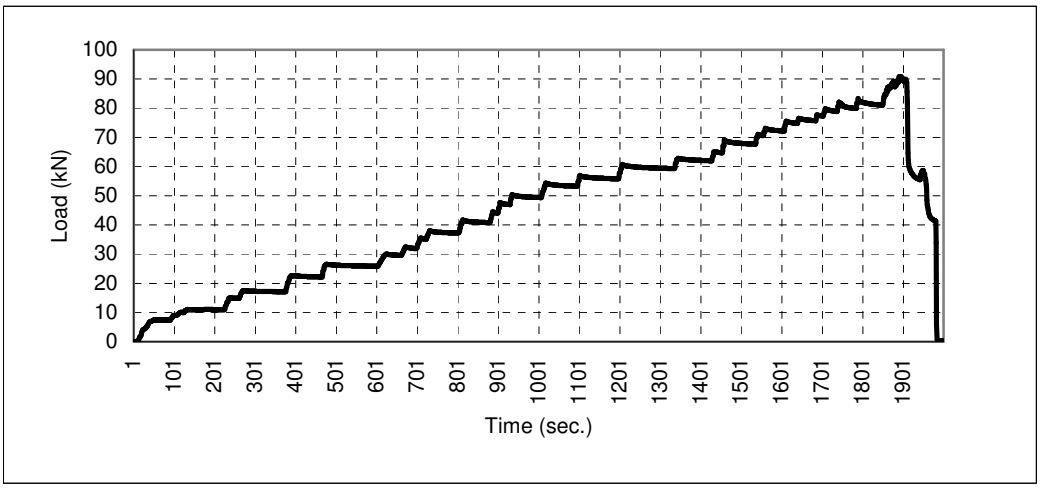

Figure 4.35. Change in load with time (BEAM-09)

Figure 4.36. Load-displacement relationship for BEAM-09

4.2.10. Specimen BEAM-10

The beam failed with flexure. For the same shear span-to-depth ratio and volume fraction, the beam with long fibres exhibited better results than short fibres. While the ultimate stress of the specimen BEAM-06 was 1.74 MPa, for the specimen BEAM-10, it was 1.80. The maximum displacement demonstrated an increase with 5.17% from 60.50 to 63.8 mm (Figure 4.40). Long fibres with volume fraction of 0.75% improved the ductility of concrete.

Figure 4.37. Crack propagation and damaged shape of the specimen BEAM-10

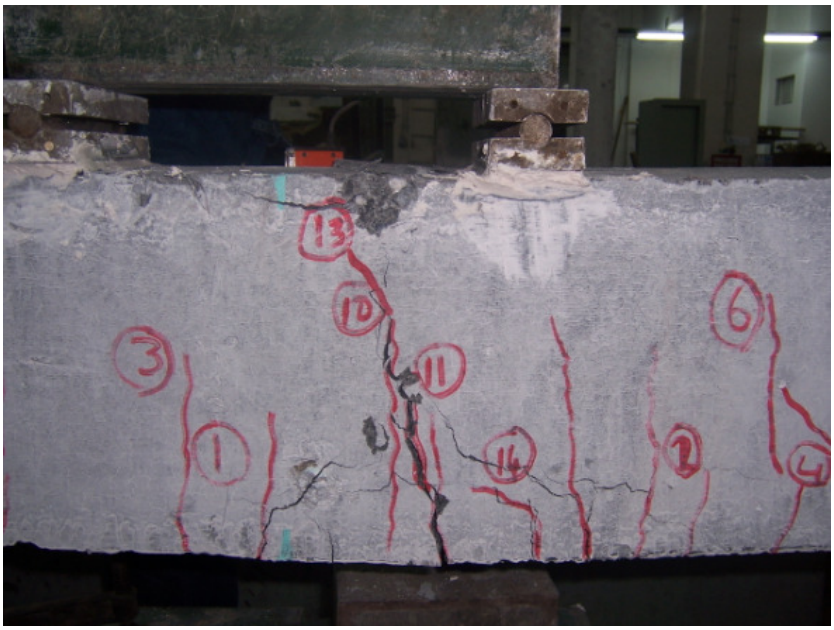

Figure 4.38. Damaged shape of the specimen BEAM-10

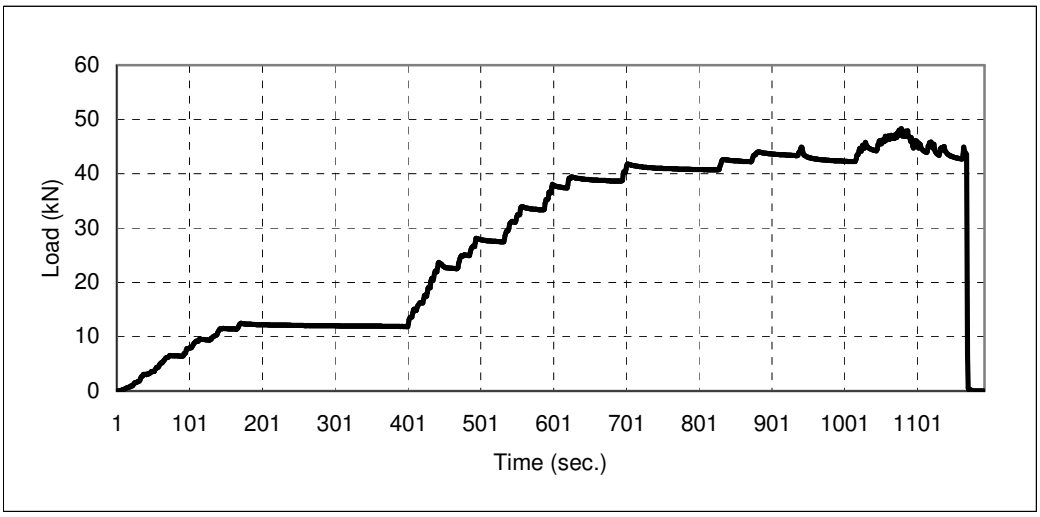

Figure 4.39. Change in load with time (BEAM-10)

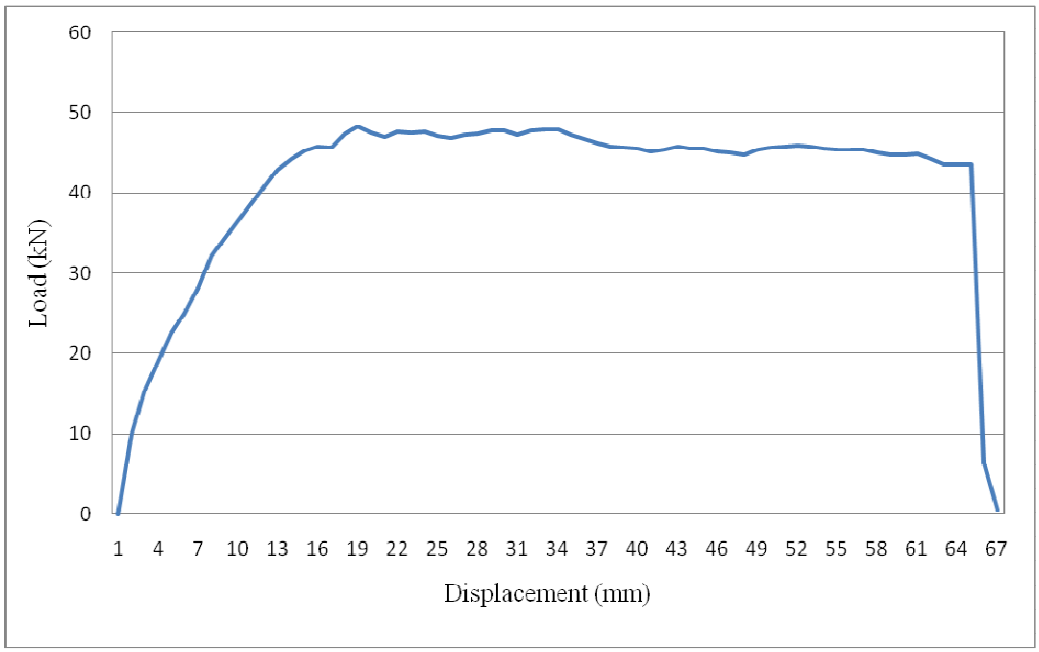

Figure 4.40. Load-displacement relationship for BEAM-10

4.2.11. Specimen BEAM-11

Since normal strength concrete without fibres was used, the load carrying capacity and displacement capacity decreased for the specimens BEAM-11 and BEAM-12. After a diagonal crack was fully developed, the beam continued to carry the increasing load. Finally, shear compression failure occurred by crushing of concrete in the compression zone (Figures 4.41 and 4.42). The cracking and ultimate stresses were 0.92 and 1.76 MPa.

When the beam reached the ultimate stress, the displacement recorded was 8.46 mm (Figure 4.44).

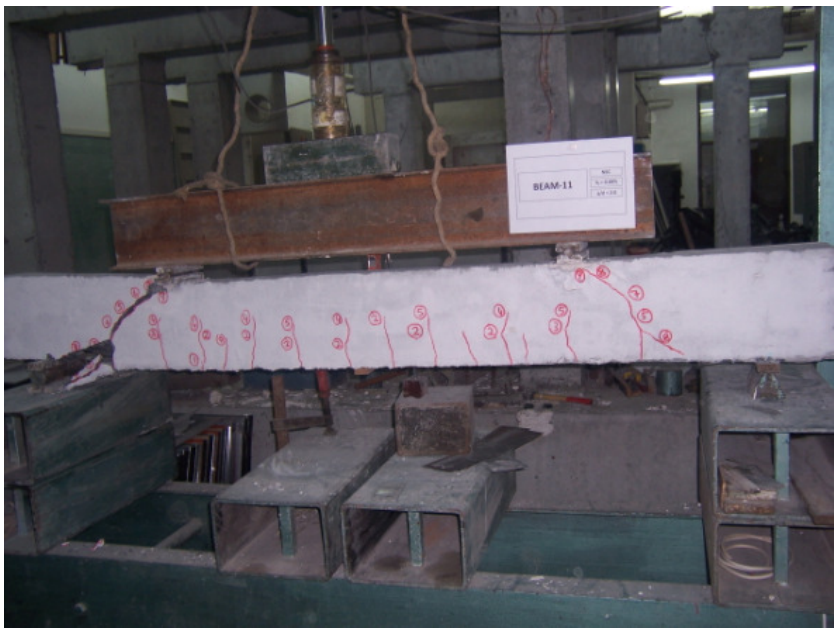

Figure 4.41. Crack propagation and damaged shape of the specimen BEAM-11

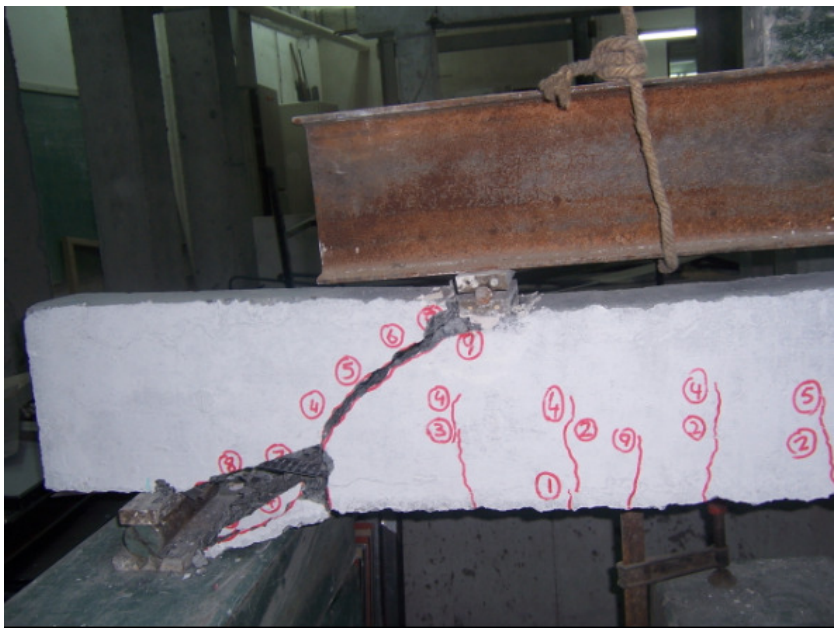

Figure 4.42. Damaged shape of the specimen BEAM-11

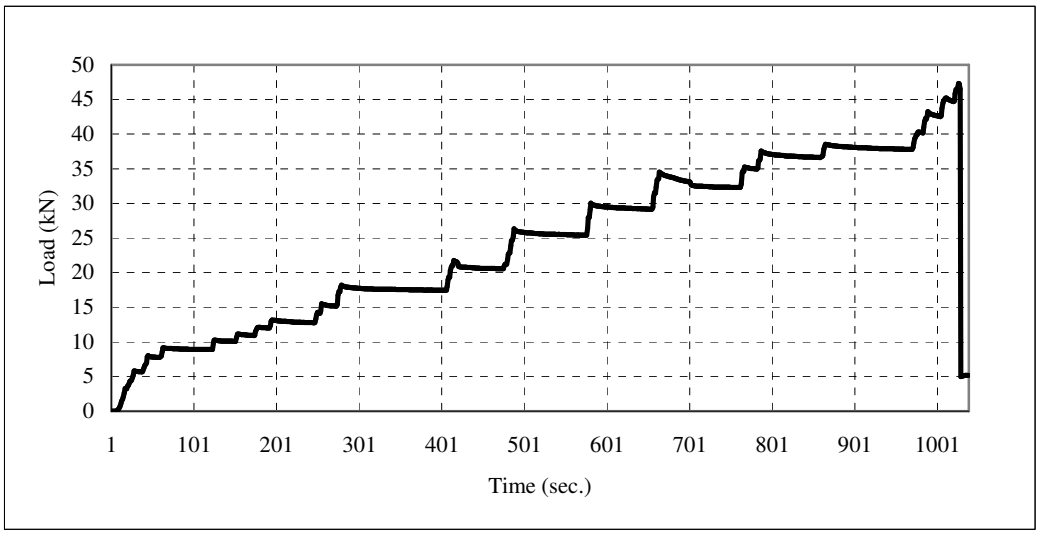

Figure 4.43. Change in load with time (BEAM-11)

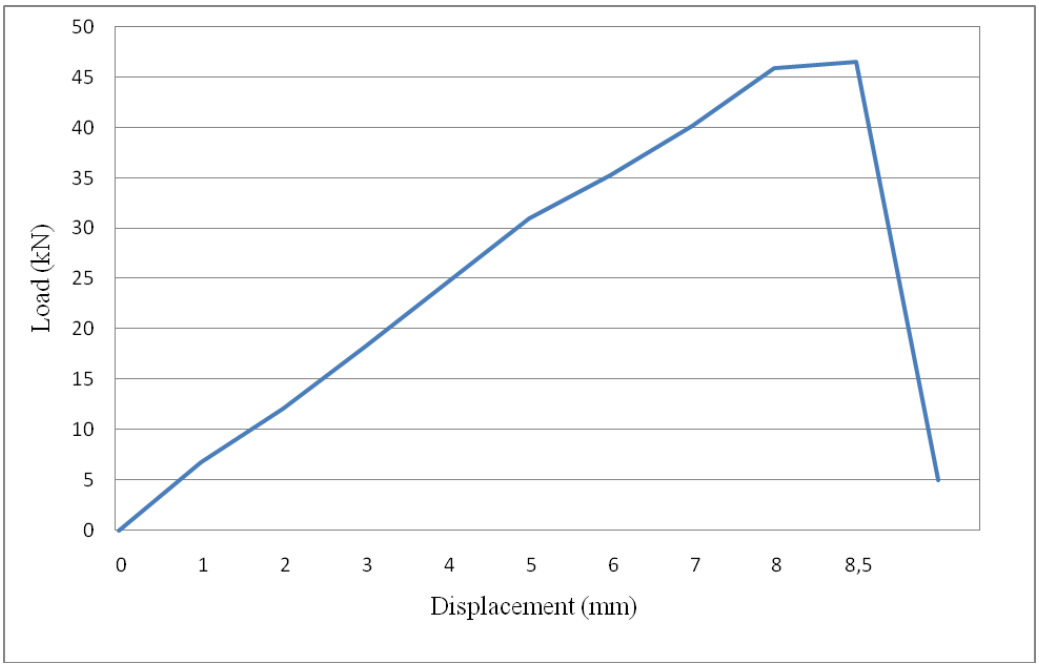

Figure 4.44. Load-displacement relationship for BEAM-11

4.2.12. Specimen BEAM-12

With the increase in load, the inclined cracks began to progress downward to the level of longitudinal steel. The beam suddenly failed across the diagonal crack (Figures 4.45 and 4.46). The cracking stress, ultimate stress and maximum displacement were 0.58 MPa, 1.23 MPa, and 6.34 mm, respectively.

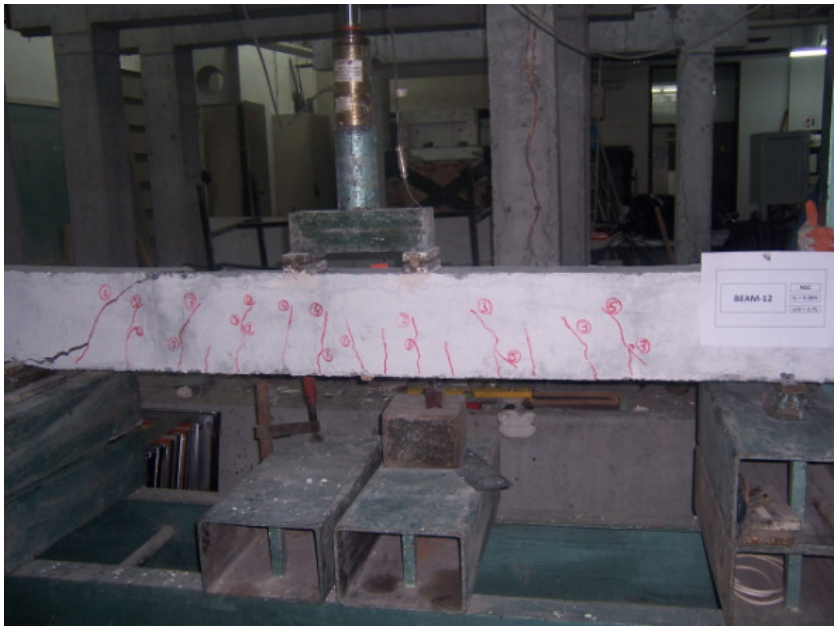

Figure 4.45. Crack propagation and damaged shape of the specimen BEAM-12

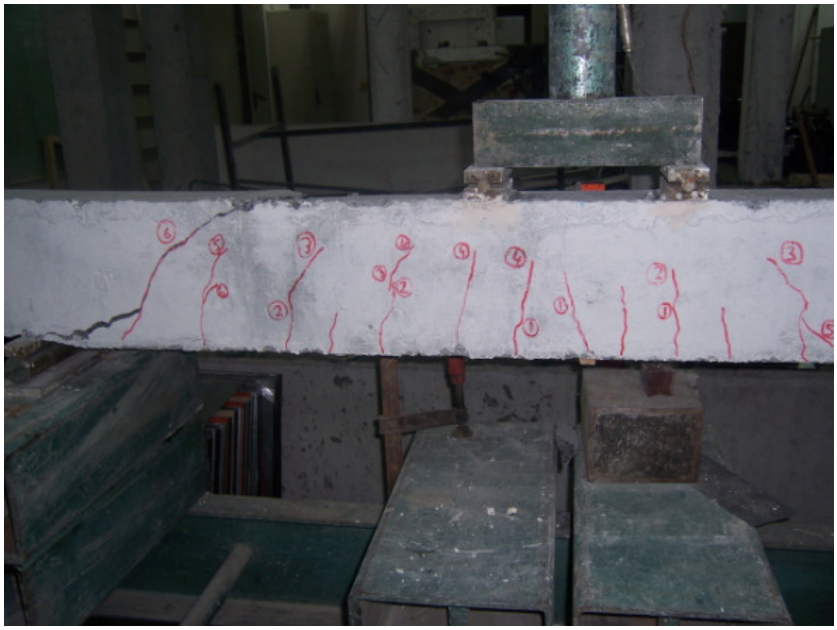

Figure 4.46. Damaged shape of the specimen BEAM-12

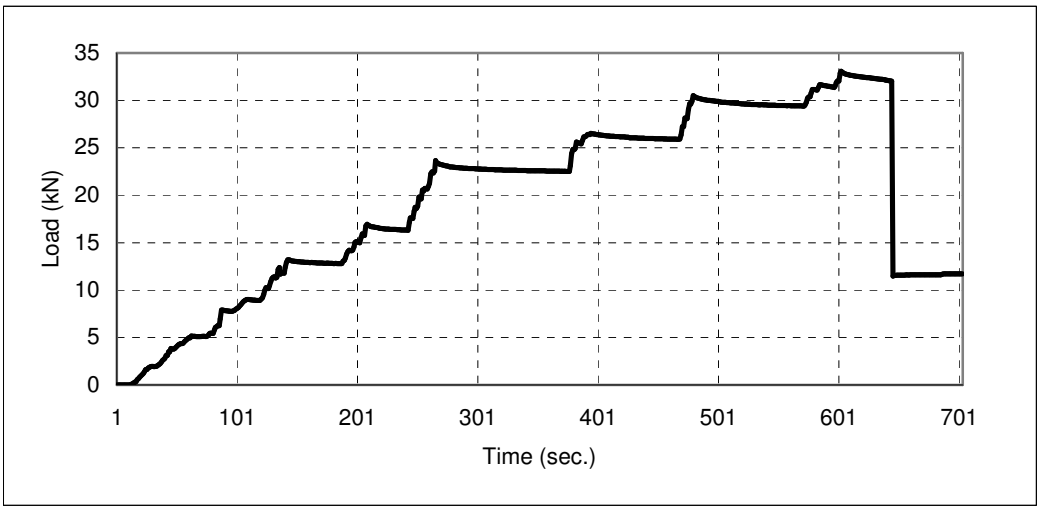

Figure 4.47. Change in load with time (BEAM-12)

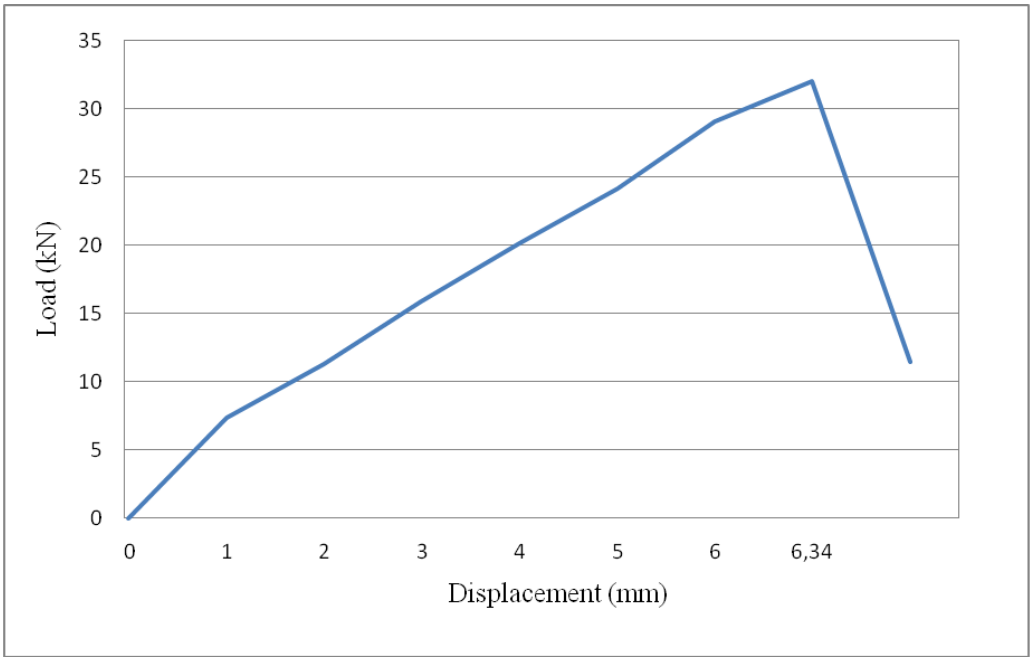

Figure 4.48. Load-displacement relationship for BEAM-12

4.3. Summary of Test Results

The cracking stresses, ultimate strengths, maximum displacements, and failure modes are reported in Table 4.1.

Table 4.1. Summary of test results

Specimen	a/d	Concrete Type	Volume Fraction (V_f,%)	Aspect Ratio	f_{ck} (MPa)	V_{cr} / b_wd (MPa)	V_u / b_wd (MPa)	Maximum Disp. (mm)	Failure Mode
BEAM-01	2.00	HSC	0.00	-	57.57	1.13	2.56	12.4	Shear Comp.
BEAM-02	3.75	HSC	0.00	-	57.57	0.78	1.27	6.62	Diagonal Tension
BEAM-03	2.00	HSC	0.50	65	60.16	1.25	2.73	12.80	Shear Comp.
BEAM-04	3.75	HSC	0.50	65	60.16	0.97	1.56	10.38	Diagonal Tension
BEAM-05	2.00	HSC	0.75	65	61.68	1.42	2.94	13.28	Shear Comp.
BEAM-06	3.75	HSC	0.75	65	61.68	1.09	1.74	60.50	Flexure
BEAM-07	2.00	HSC	0.50	80	60.86	1.34	2.94	13.40	Shear Comp.
BEAM-08	3.75	HSC	0.50	80	60.86	0.89	1.39	12.80	Diagonal Tension
BEAM-09	2.00	HSC	0.75	80	63.59	1.58	3.38	57.34	Flexure
BEAM-10	3.75	HSC	0.75	80	63.59	1.18	1.80	63.80	Flexure
BEAM-11	2.00	NSC	0.00	-	42.58	0.92	1.76	8.46	Shear Comp.
BEAM-12	3.75	NSC	0.00	-	42.58	0.58	1.23	6.34	Diagonal Tension

4.4. Discussion of Test Results

4.4.1. Influence of Shear Span-to-Depth Ratio on Shear Resistance

Except the specimen BEAM-09, all beams with *a/d* = 2 failed in shear compression, which corresponded in each case to a brittle failure along a single shear crack. For the specimen BEAM-09, 0.75% RC-80/60-BN fibre content increased the ductility and caused flexural failure with crushing of concrete in compression zone. The maximum stress value (3.38 MPa) was recorded. While it was expected to fail in shear, the specimen behaved like a well-confined beam. The capacity of the beams increased with 24.3% for the high-strength concrete specimens (BEAM-01 and BEAM-09). For the specimens with *a/d* = 2, the typical load-deflection histories are shown in Figure 4.49.

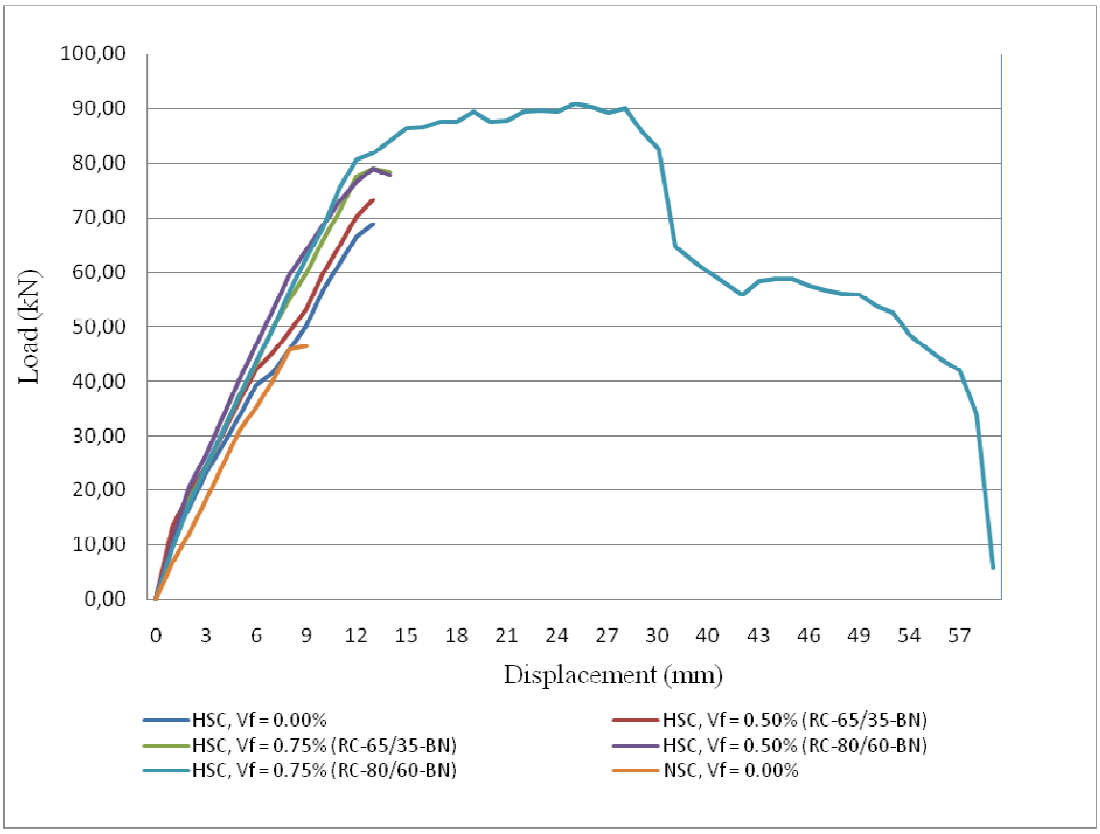

Figure 4.49. Load-displacement relationship for the specimens with *a/d* = 2

For the specimens with *a/d* = 3.75, diagonal tension and flexure dominated failures were observed. Four of the beams failed with diagonal tension and the other two with flexure. The specimens exhibited flexural behavior were BEAM-06 and BEAM-10 having the same volume fraction (V_f = 0.75%), but different fibre types. Because these two beams failed in flexure, the ultimate load was not equal to the shear strength of the beams. The deflection values were over 60 mm due to the contribution of longitudinal reinforcement. For the other 4 beams, sudden failures with the diagonal crack extending into the compression zone occurred.

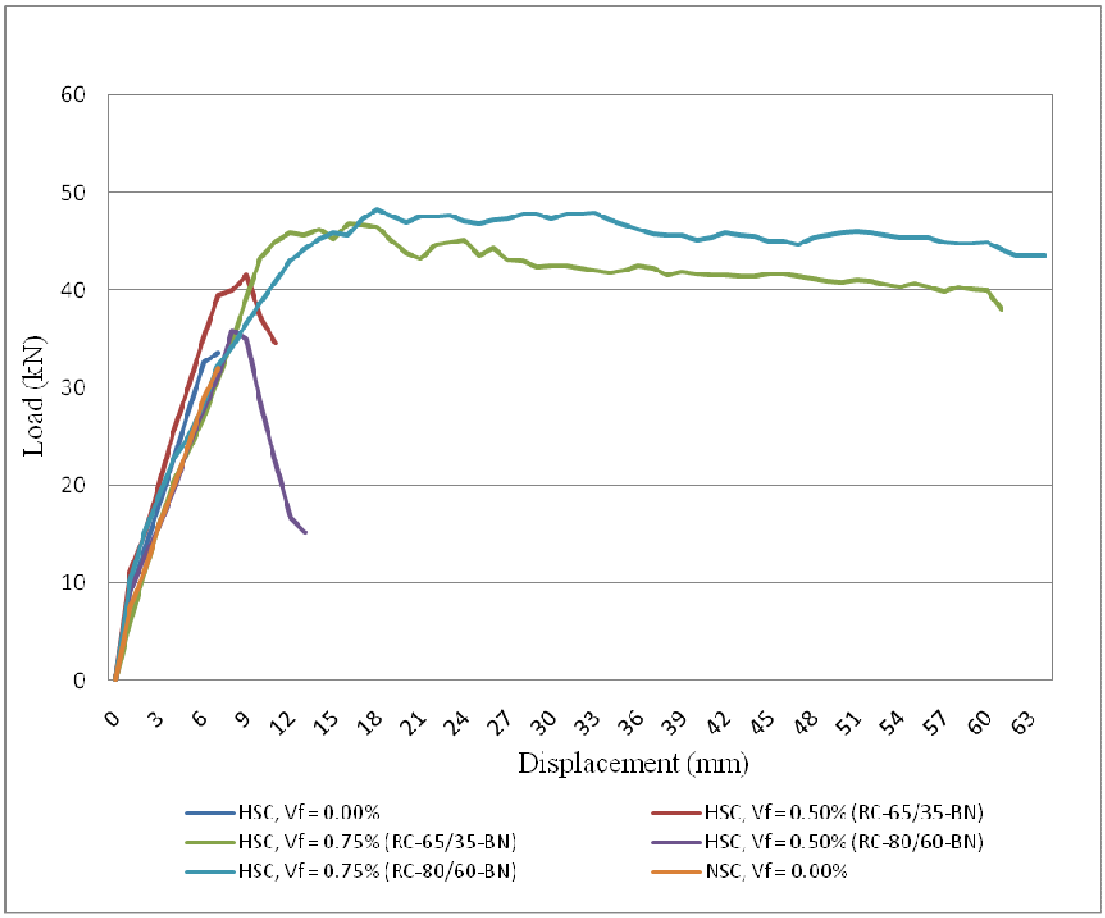

Figure 4.50. Load-displacement relationship for the specimens with *a/d* = 3.75

For the fibre-reinforced concrete specimens, the difference in capacity between the beams with low shear span-to-depth ratios was smaller than the difference between the beams with large shear span-to-depth ratios. While the maximum increase in the strength was low (15 to 32%) for the beams with *a/d* = 2, the increase ranged from 37 to 42% for the beams with *a/d* = 3.75, which are more typical in practice. Although the effectiveness of dowel action and arching action decreased with increasing shear span-to-depth ratio, the difference in capacity increased.

On the other hand, for the specimens without fibres, the change in the capacity of the beams with *a/d* = 2 was %45, while it was 3% for the beams with *a/d* = 3.75. The difference in the results of the beams with and without fibres demonstrates that fibres are more effective for the beams with large shear span-to-depth ratios. The change in shear strength with different shear span-to-depth ratios is shown in Figure 4.51.

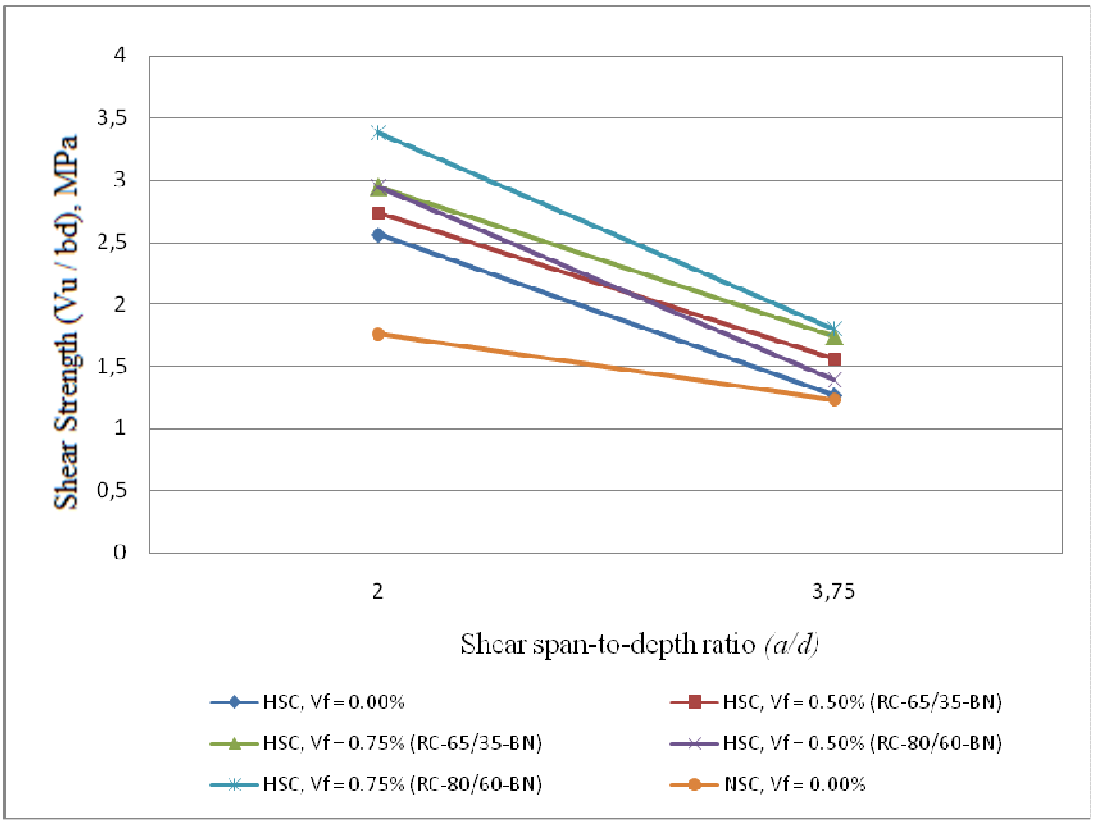

Figure 4.51. Shear span-to-depth effect on shear resistance

The cracking shear stress decreased with increasing shear span-to-depth ratio; it increased with increasing volume fraction; and it increased with increasing strength of concrete (Figure 4.52). The fibres were effective in delaying the formation of cracks, or at least in restricting their initial growth. The cracking stress values of the specimens with the RC-80/60-BN fibres were larger than the values of the RC-65/35-BN fibre-reinforced concrete specimens.

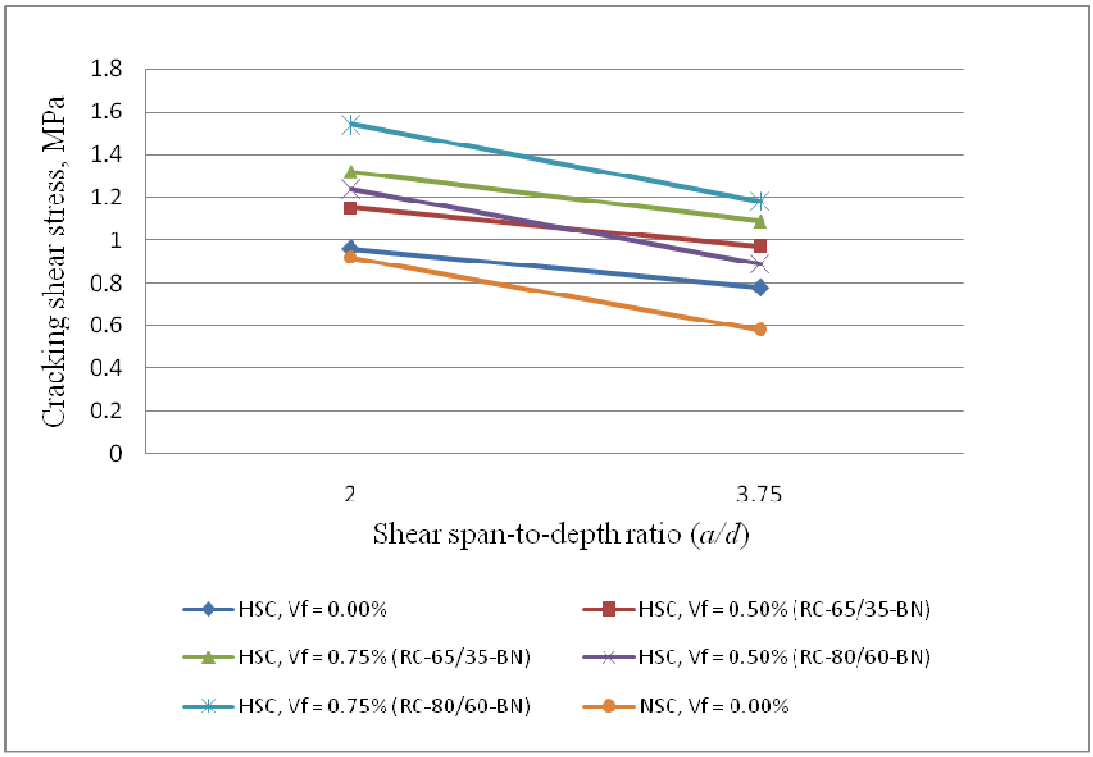

Figure 4.52. Shear span-to-depth effect on cracking stress

4.4.2. Effect of Concrete Strength

It is known that the increase in the strength of concrete improves the shear resistance of beams. The tensile strength of concrete is given as a function of compressive strength in many standards. Therefore, for the same conditions, the capacity of high strength concrete members is larger than the capacity of the members with normal concrete. In the tests, the effect of the strength of concrete was observed. The strength of concrete is more effective on shear behavior for a/d = 2 than a/d = 3.75. The shear strength of the specimens without fibres increased with 45.5% for a/d = 2 and 3.3% for a/d = 3.75.

4.4.3. Influence of Fibre Type and Volume Fraction

The increasing steel fibre volume greatly increased the capacity of the beams. While the failure mode was shear compression or diagonal tension for the beams without fibres, with increasing fibre volume, it changed to a combination of shear and flexure or pure flexure. The cracks dominated by shear or flexure were spaced more closely as the volume fraction increased.

For the specimens strengthened by the RC-65/35-BN fibres with a fibre content of 0.50%, the strength of the beams increased with 7% for *a/d* = 2 and 23% for *a/d* = 3.75. As the steel fibre volume increased to 0.75%, differences in capacity for *a/d* = 2 and 3.75 were 15% and 37%, respectively. For *a/d* = 2, all beams failed with shear. For *a/d* = 3.75, as the beams without fibre and with a fibre volume of 0.50% failed with diagonal tension, the specimen BEAM-06 with a fibre volume of 0.75% exhibited flexural behavior with an ultimate displacement of 60.50 mm.

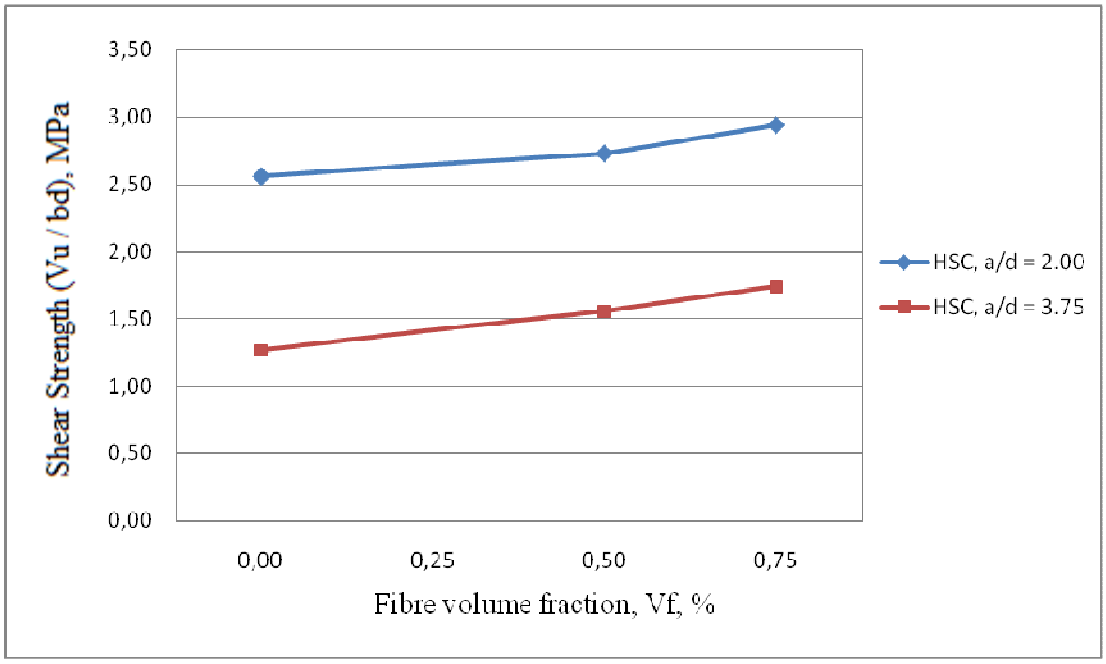

Figure 4.53. Influence of volume fraction on shear strength (RC-65/35-BN)

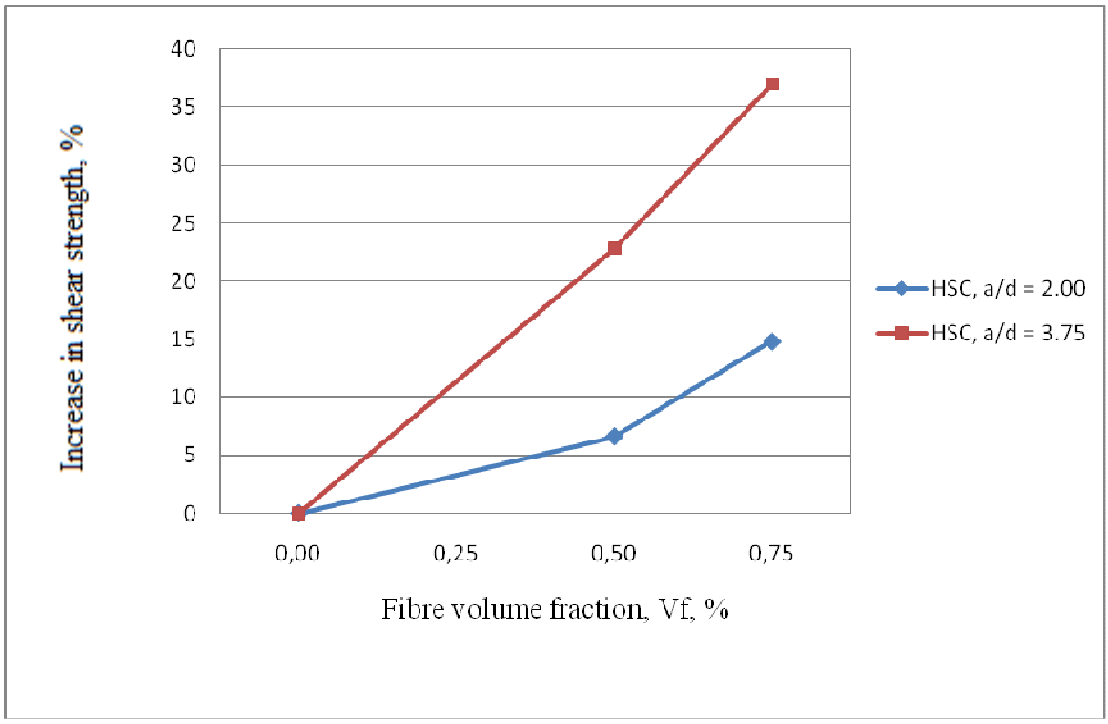

Figure 4.54. Increase in shear strength with change in volume fraction (RC-65/35-BN)

For the specimens reinforced by the RC-80/60-BN fibres with a fibre volume of 0.50%, the shear carrying capacity of the specimens increased with 15% for *a/d* = 2 and 10% for *a/d* = 3.75. With further increase in volume fraction (0.50 to 0.75%), the strength of the beams increased with 32% and 42% for *a/d* = 2 and 3.75, respectively. For *a/d* = 2, while the beams without fibre and with a volume fraction of 0.50% failed with shear, BEAM-09 (V_f = 0.75%) showed flexural behavior. For *a/d* = 3.75, as the beams without fibre and with a fibre volume of 0.50% failed with diagonal tension, the specimen BEAM-10 failed with flexure with an ultimate displacement of 63.80 mm, which is the highest displacement value in the tests.

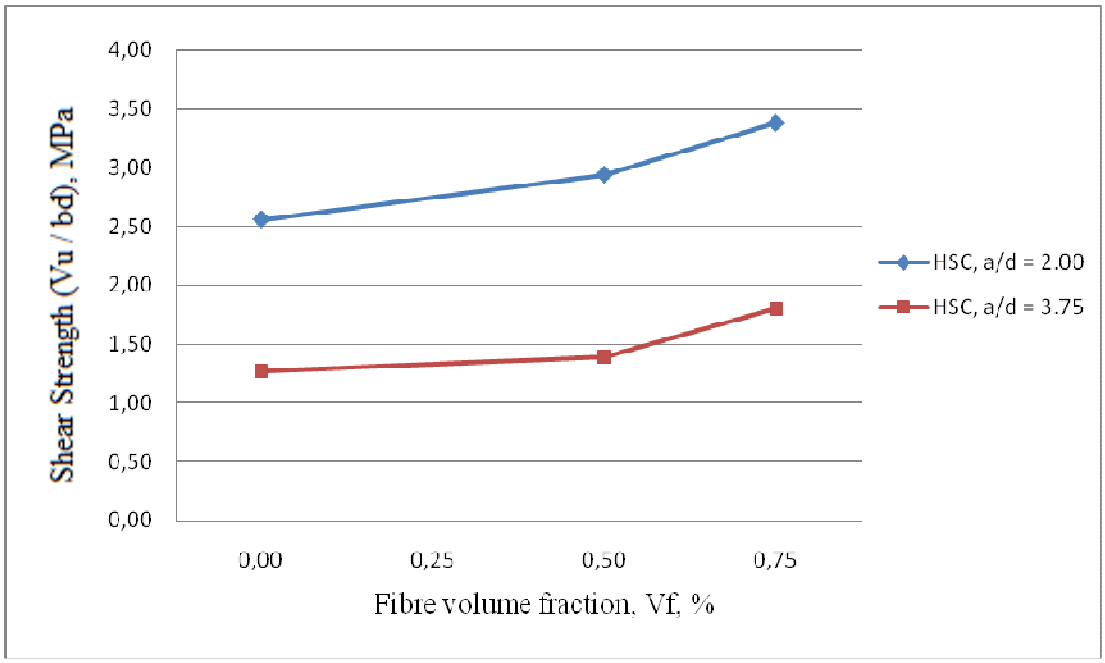

Figure 4.55. Influence of volume fraction on ultimate shear stress (RC-80/60-BN)

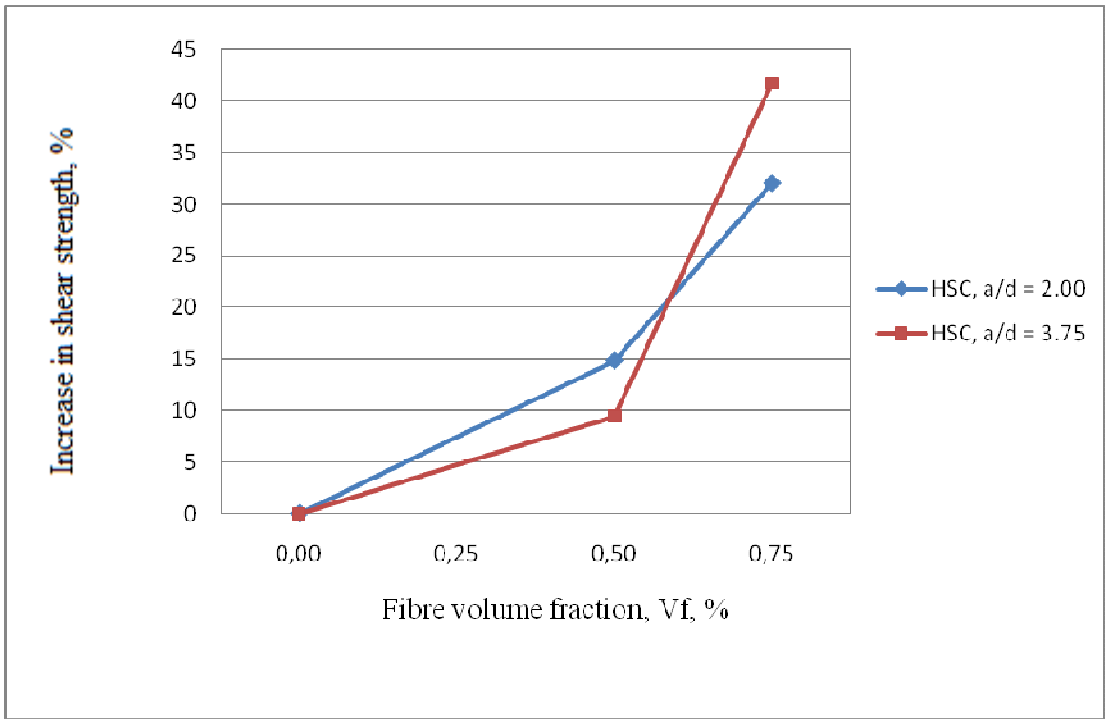

Figure 4.56. Increase in shear strength with change in volume fraction (RC-80/60-BN)

The RC-80/60-BN fibres gave better results than the RC-65/35-BN fibres. For the fibre content of 0.50%, the beams with RC-80/60-BN fibres exhibited extra 8% strength for *a/d* = 2. When the fibre content increased to 0.75%, the specimens strengthened by the RC-80/60-BN fibres also showed extra 15% strength for *a/d* = 2 and %4 for *a/d* = 3.75.

For *a/d* = 2, as the failure mode of the specimen BEAM-05 with an RC-65/35-BN fibre volume of 0.75% was shear compression, the specimen BEAM-09 strengthened by RC-80/60 fibres failed with flexure. For the fibre content of 0.75% and *a/d* = 3.75, both of the specimens (BEAM-06 and BEAM-10) failed with flexure with high deflection values.

4.5. Comparison of Test Results and Previous Studies

The wide study on the shear behavior of reinforced concrete beams with and without fibres indicates that the nominal stress at shear cracking and the ultimate shear strength increase with decreasing shear span-to-effective depth ratio and increasing concrete compressive strength, longitudinal reinforcement ratio, and fibre volume fraction. These experimental studies demonstrated that steel fibres have significant influence on shear resistance. It is recommended in the studies that steel fibres can replace the conventional web reinforcement in beams.

According to the study made by Salna and Marciukaitis [14], the difference in the increase of shear carrying capacity increased with decreasing shear span-to-depth ratio. They chose three span-to-depth ratios (1, 1.5, and 2) and three volume fractions (1, 1.5, and 2%). In this study, results inversely showed that the difference in ultimate shear strength increased with increasing *a/d* ratio. While the change in shear strength with a fibre volume of 0.75% ranged from 15 to 32%, according to the Salna and Marciukaitis' study, the increase in shear strength was 14% for *a/h* = 2 and V_f = 1%.

For a fibre volume of 0.75%, the three of four specimens (two beams with a/d = 3.75 and one with a/d = 2) exhibited flexural behavior similar to the results of the study of Montesinos and Gustavo [11]. Their study supported the use of steel fibres as an alternative to minimum transverse shear reinforcement (stirrups or hoops) for beams. They also recommended a minimum volume fraction of 0.75% as minimum shear reinforcement because all beams contained $V_f \geq 0.75\%$ exhibited a shear stress at failure greater than the conservative lower bound value. Greenough and Nehdi [19] also recommended the fibre content of 0.75% as minimum shear reinforcement. They also stated that 1.0% fibre volume can be chosen as optimum shear reinforcement in beams.

There is no satisfying information about the efficiency of type, aspect ratio or length of fibres. It is indicated in this study that the aspect ratio or the length of fibres influences the shear strength of beams. The fibres that have larger aspect ratios and lengths improve the shear resistance of beams. Greenough and Nehdi [19] stated in their study that fibres with hooked or flat end have greater influence on shear resistance than wavy fibres. It is recommended to make further investigations about the efficiency of aspect ratio and fibre length.

5. CONCLUSIONS

The experimental results exhibit the influence of shear span-to-depth ratio (a/d); steel fibre volume fraction; fibre type; and the strength of concrete on the onset of cracking, shear strength, ultimate deflection, and failure mode. The following conclusions and key findings can be drawn on the basis of the results presented in this study:

Both the first crack strength and ultimate shear strength increase with decreasing *a/d* ratio. The ultimate stresses of the beams with a/d = 2 were particularly larger (43 to 112%) than the ultimate stresses of the beams with *a/d* = 3.75. The increase in the strength ranged from 15 to 32% for the beams with *a/d* = 2 as the increase was large (37 to 42%) for the beams with *a/d* = 3.75. The difference in the results of the beams with and without fibres demonstrates that fibres are more effective for the beams with large shear span-to-depth ratios. For *a/d* = 2, except one beam, all beams failed in shear. On the other hand, even with small shear span-to-depth ratios, the beams with high volume fraction (0.75%) of long fibres exhibited flexural behavior. When shear span-to-depth ratio increased from 2 to 3.75, the failure modes were diagonal tension and flexure. The deformation capacity decreases with large shear span-to-depth ratios.

The results clarify the enormous influence of steel fibres on ductility, cracks propagation, and the shear capacity of beams. The addition of steel fibres decreases crack spacing and widths, increases deformation capacity, and may change a brittle mode at failure to a ductile mode. While the failure mode is shear compression or diagonal tension for the beams without fibres, with the addition of fibres with high volume fraction (0.75%), it changes to a combination of shear and flexure or pure flexure. Steel fibres with a fibre volume of 0.75% behave like minimum shear reinforcement for beams

Long fibres are more effective on shear resistance than short ones. For the specimens strengthened by the RC-65/35-BN fibres with a volume fraction of 0.75%, the strength of the beams increased with 15% for *a/d* = 2 and 37% for *a/d* = 3.75. For the same fibre content, the shear carrying capacity of the RC-80/60-BN fibre-reinforced specimens increased with 32% for *a/d* = 2 and 42% for *a/d* = 3.75. While all other beams with *a/d* = 2

failed in shear, one of the specimens with RC-80/60-BN fibres (V_f = 0.75%) exhibited flexural behavior. Even with small shear span-to-depth ratios, long fibres with a fibre volume of 0.75% act like web reinforcement. The fibre volume fraction of 0.75% is recommended as minimum shear reinforcement for beams. The addition of long steel fibres changes a brittle failure to a ductile behavior. Further study on the beams strengthened by long fibres with larger volume fractions is recommended.

The increase in the compressive strength of concrete improves the shear resistance of beams. The capacity of high strength concrete members is larger than the capacity of the members with normal concrete. Concrete strength is more effective on shear behavior for specimens with a/d = 2 than specimens with a/d = 3.75. In the tests, the shear strength of the specimens without fibres increased by 45.5% for specimens with a/d = 2, but only 3.3% for specimens with a/d = 3.75.

REFERENCES

1. Wang, C. and C. G. Salmon, *Reinforced Concrete Design*, Text Book, Longman Higher Education, University of Wisconsin, USA, 1979.

2. Mphonde, A. G. and G. C. Frantz, "Shear Tests of High and Low Strength Beams without Stirrups", *ACI Journal*, Vol. 81, No. 4, pp 350-357, London, 1984.

3. Ersoy, U., *Reinforced Concrete*, Text Book, Middle East Technical University, Turkey, 1994.

4. Mays, G.C. and R.A. Barnes, *The Shear Strengthening of Rectangular Reinforcement Concrete Beams Using Bonded External Reinforcement*, Technical Report, Cranfield University, UK, 1995.

5. Kutzing, L., *Shear Strength of Steel Fibre Reinforced Concrete Beams and Plates*, Technical Report, University of Leipzig, Germany, 1997.

6. Dramix*, Design Procedures for Dramix Steel Fibre-Reinforced Concrete*, Design Catalog, 2001.

7. Musluer, L., *Analysis of Reinforced Concrete Beams to Shear Failure*, M.S. Thesis, Department of Civil Engineering, Boğaziçi University, 2003.

8. Lofgren, I., *Fibre-reinforced Concrete for Industrial Construction*, Ph.D. Thesis, Department of Civil and Environmental Engineering, Chalmers University of Technology, Sweden, 2005.

9. Tan, K. H. and M. K. Saha, *Ten-Year Study on Steel Fiber-Reinforced Concrete Beams under Sustained Loads*, Vol. 102, No. 3, USA, May-June 2005, pp. 472-480, 2005.

10. Majdzadeh, F., Soleimani, S. M. and N. Banthia, “Shear strength of reinforced concrete beams with a fiber concrete matrix”, *Canadian Journal of Civil Engineering*, Volume 33, Number 6, pp. 726-734, 2006.

11. Montesinos, P. and J. Gustavo, "Shear strength of beams with deformed steel fibres", *Concrete International*, Michigan, USA, 2006

12. Bukhari, I. A. and S. Ahmad, *Evaluation of Shear Strength of High-Strength Concrete Beams without Stirrups*, Technical Report, Civil Engineering Department, University of Engineering and Technology, Pakistan, 2007.

13. Madan, S. K., Kumar, G. R. and S. P. Singh, *Steel Fibres as Replacement of Web Reinforcement for RCC Deep Beams in Shear*, Technical Report, India, 2007.

14. Salna, R. and G. Marciukaitis, *The Influence of Shear Span Ratio on Load Capacity of Fibre Reinforcement Concrete Elements with Various Steel Fibre Volumes,* Technical Report, Department of Reinforced Concrete and Masonry Structures, Vilnius Gediminas Technical University, Lithuania, 2007.

15. Shah, A. and S. Ahmad, *An Experimental Investigation into Shear Capacity of High Strength Concrete Beams*, Technical Report, Department of Civil Engineering, University of Engineering and Technology, Pakistan, 2007.

16. Sun, S. and D. A. Kuchma, *Shear Behavior and Capacity of Large-Scale Prestressed High-Strength Concrete Bulb-Tee Girders,* Technical Report, Department of Civil and Environmental Engineering, University of Illinois, Urbana-Champaign, 2007.

17. TS-500, *Betonarme Yapıların Hesap ve Yapım Kuralları*, Turkish Standards, 2007.

18. Arslan, G., “Cracking Shear Strength of RC Slender Beams without Stirrups”, *Journal of Civil Engineering and Management,* Istanbul, Turkey, 2008.

19. Greenough, T. and M. Nehdi, “Shear behavior of Fiber-Reinforced Self-Consolidating Concrete Slender Beams”, *ACI Material Journals*, Canada, 2008.